Analyzing & Determining the Structure of Penicillin Binding Protein 5 from *Enterococcus faecium*

By

Christopher Lee

B.S., University of Michigan, 2015

Thesis

Submitted in partial fulfillment of the requirements for the

degree of Master of Science in the Department of Molecular Pharmacology,

Physiology and Biotechnology at Brown University

PROVIDENCE, RHODE ISLAND

May 2017

AUTHORIZATION TO LEND AND REPRODUCE THESIS

As the sole author of this thesis, I authorize Brown University to lend it to other institutions or individuals for the purpose of scholarly research.

Date:_____ Signature: _____
Christopher Lee, Author

I further authorize Brown University to reproduce this thesis by photocopying or other means, in total or in part, at the request of other institutions or individuals for the purpose of scholarly research.

Date:_____ Signature: _____
Christopher Lee, Author

This thesis by Christopher Lee is accepted in its present form by the

Department of Molecular Pharmacology, Physiology, and Biotechnology as satisfying

the thesis requirements for the degree of Master of Science

Date: _____ Signature:_____
Dr. Wolfgang Peti, Advisor

Date: _____ Signature:_____
Dr. Jacquelyn Schell, Reader

Date: _____ Signature:_____
Dr. Edith Mathiowitz, Reader

Approved by the Graduate Council

Date: _____ Signature: _____
Dr. Andrew G. Campbell, Dean of the Graduate School

Acknowledgements

I would like to start off by thanking my adviser, Dr. Wolfgang Peti, for giving me the opportunity to work as a member of his laboratory. Under his guidance, I gained a plethora of knowledge and experiences that has helped me grow as an aspiring scientist. I would also like thank Dr. Thomas Moon for his mentorship during the duration of the project. He was an excellent instructor who pushed me to make the best out of this opportunity. Dr. Rebecca Page, for showing me the ropes on crystallization and structural analysis, which were key aspects of my project. As well as for being a wonderful instructor. Dr. Louis B. Rice and Charlene Desbonnet, for collaborating with us and providing resources that helped push this project forward. Dr. Jacquelyn Schell, for her patience and support during my time within the program and giving great counsel. Dr. Edith Mathiowitz, for her passion in helping her students reach success. Finally, I'd like to thank the members of the Peti and Page lab, especially Xinru Wang and Jocelyn Newton, for promoting an enthusiastic and encouraging environment that helped me enjoy every day of working at the Peti lab.

I'd also like to thank my mom, my dad, and my sister Joanne Lee, for their undying love and support while completing this thesis. Without them, none of this would be possible. I am also incredibly thankful for the amazing support and inspiration from my friends and colleagues, especially Kara Ford and Amen Okundaye, for always being there and for helping me have a wonderful graduate school experience.

Table of Contents

Table of Figures

Abstract

Penicillin Binding Protein 5 (PBP5) is a membrane bound transpeptidase that plays an important role in β-lactam antibiotic resistance in *Enterococcus faecium*. Normally, β-lactams inhibit the transpeptidase activity of Penicillin Binding Proteins (PBPs) by way of irreversible acylation of the antibiotic to an active site serine. However, the PBP of *E. faecium* (PBP5) has been observed to be unaffected by β-lactam inhibition and continues to function as a transpeptidase. Studying this enzyme is important in understanding the steps taken in these unique resistance mechanisms, which can be beneficial in future drug design strategies.

Here, we report the crystal structure of PBP5, which displays a highly conserved active site within the C-terminal domain. Through various protein purification techniques and X-ray crystallography, we were able to determine the structure of PBP5 at a resolution of 2.7 Å. We also report the crystal structures of β-lactam acyl-enzyme complexes PBP5:Penicillin G and PBP5:Imipenm, which were solved at a resolution of 2.9 Å and 2.8 Å, respectively. Structural alignment and analysis revealed small structural differences between the PBP5 apo structure and each respective acyl-enzyme complex, displaying the ineffectiveness of antibiotics on PBP5.

We also observed similarities between PBP5 and another PBP known as PBP2a of *Staphylococcus aureus.* PBP2a is also known to be resistant towards β-lactam antibiotics. Superposition of PBP5 and PBP2a revealed a highly conserved active site in both structures as well as similar active site interactions with Penicillin G. This could indicate a resistance mechanism that is shared between both PBPs. Despite a highly conserved active site; sequence and structural alignments denote a high degree of variability between both enzymes. Most notably, the structure of PBP5 reveals no current evidence of an allosteric region within its structure, unlike the reported structure of PBP2a that suggests the presence of an allosteric site.

Background

The Antibiotic Resistance Crisis

Antibiotics are regarded as one of the major innovations of modern medicine. They have made a beneficial impact upon human health by increasing life spans and improving traditional medical practices such as organ transplantations and chemotherapy. In parts of the world where resources are thin, antibiotics are the main cause behind decreasing mortality rates from "poverty-related infections" [1]. However, due to their high demand worldwide, antibiotics have lost their effectiveness. Overuse and the lack of research in developing new antibiotics, have assisted in the development of antibiotic resistance. The situation gained much attention to the point where the Center of Disease Control declared that humanity was now entering a Post-Antibiotic Era [2]. Dr. Margaret Chan, Director General of the World Health Organization, describes the "post-antibiotic era" as "an end to modern medicine as we know it. Things as common as strep throat or a child's scratched knee could once again kill [3]."

The Pre-Antibiotic Era

Death by infection, as mentioned by Dr. Margaret Chan, was a normal occurrence during the "pre-antibiotic era" [4]. Today, bacterial meningitis can easily be treated with antibiotics. However, during the "pre-antibiotic era" where antibiotics were nonexistent, over 90% of children in the United States died from it. Of those who lived, most were severely disabled. Bacterial species were reproducing at an alarming rate, leading to significant increases in child mortality during the "pre-antibiotic" era [5]. They also caused a negative impact along the frontlines of the battlefield. Diaries of doctors who treated soldiers during the First World War

revealed the challenges they faced in fighting infections. Cultures of wound swabs were taken from injured soldiers, with results showing 90.3% of wounds being infected [6]. Ten newly formed bacteria were discovered from a single patient's injury [7]. With these complications circulating around the battlefield, effective treatment was in high demand.

The Accidental Discovery

Luckily, this demand was met by a simple act of carelessness from Sir Alexander Fleming. Known to be an irresponsible lab technician, Fleming discovered mold growing on an accidentally contaminated staphylococcus culture plate. After further investigation, he observed how staphylococci growth was stunned. His account from the British Journal of Experimental Pathology reads, "The staphylococcus colonies became transparent and were obviously undergoing lysis… the broth in which the mold had been grown at room temperature for one to two weeks had acquired marked inhibitory, bactericidal and bacteriolytic properties to many of the more common pathogenic bacteria [8]." Eventually, his research was used to produce penicillin in medicinal form, becoming available for distribution in 1942. It was first used to successfully treat a patient with streptococcal septicemia.

The discovery of penicillin drastically changed the landscape of medicine. Infections that once led to an inevitable death, such as bacterial meningitis and endocarditis, could easily be treated with penicillin. Without the development of penicillin and other newly designed antibiotics, soldiers would suffer from fatal injuries. Once penicillin became high in demand, many pharmaceutical companies began searching for other natural products that displayed antibacterial activity. This led to the development of many different kinds of antibiotics such as streptomycin, aminoglycosides, and tetracyclines.

Causes of Antibiotic Resistance

Despite the benefits of penicillin, Sir Alexander Fleming warned of the consequences of overuse. He warned that the "public will demand [the drug and] …. Then will begin an era … of abuses [9]." Unfortunately, Sir Alexander Fleming's warning became a foreshadowing of today's documented abuse. Overuse of antibiotics drives the evolution of antibiotic resistance, where in some cases, horizontal gene transfers could allow antibiotic resistance to be transferred between several species of bacteria. Epidemiological studies have shown a clear correlation between antibiotic consumption and the emergence of resistant bacteria strains [10]. Mutations have the potential to cause spontaneous occurrences of resistance as well. By eliminating drug-sensitive competitors, antibiotics consequently leave behind resistant bacteria that are capable of reproducing [9]. Despite the studies and proven evidence of the dangers regarding overuse, antibiotics continue to be overprescribed [10].

Another contributing factor behind resistance development is the lacking availability of new antibiotics. The absence of newly manufactured antibiotics is the result of their current perception of being low in value. While one could argue that being inexpensive was a benefit, pharmaceutical companies saw that antibiotic development was "no longer considered to be an economically wise investment [11]." Their short-term effectiveness led to a reputation of being an unprofitable drug compared to drugs that treat long-term illnesses or chronic diseases. This deficiency in new and effective antibiotics allows for multidrug resistant bacteria to continue to rise and cause multiple deaths around the world. In fact, per the Review on Antimicrobial Resistance, if there continues to be a lack of initiative in this area of research, it was extrapolated that someone could die every three seconds from antibiotic resistance by the year 2050 (See

Figure 1), resulting in the deaths of 10 million people per year [12].

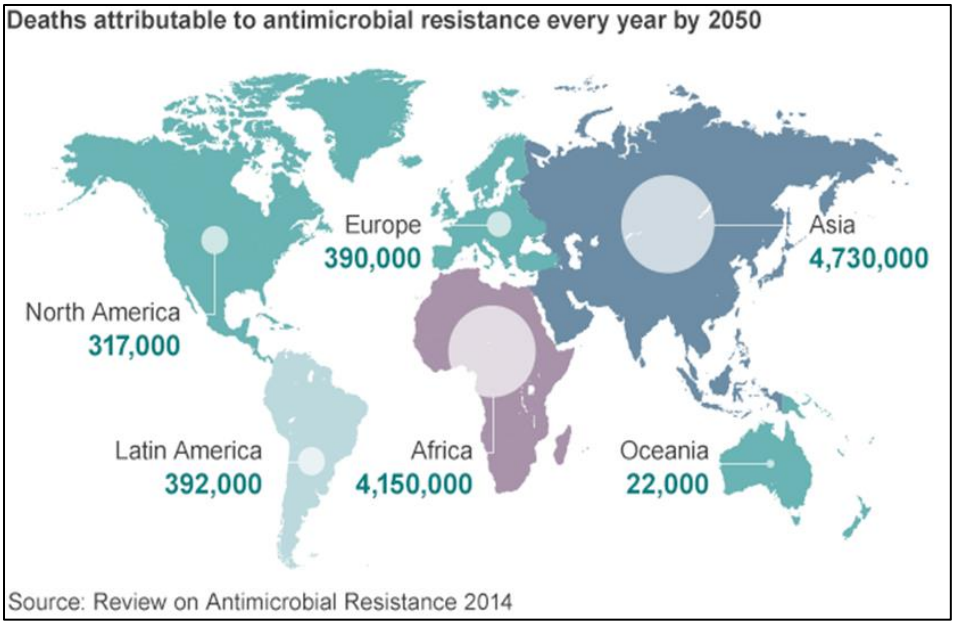

Figure 1: The global picture of deaths by continent from antimicrobial resistance (11)

MRSA and VRE lead the way

The two species that largely contribute to the threat of antibiotic resistance are *Staphylococcus aureus* and Enterococcus species such as *Enterococcus faecium*. *S. Aureus*, in its methicillin resistant form, has killed more Americans each year than "HIV/AIDS, Parkinson's disease, emphysema, and homicide combined [13]." MRSA infections are the most common of all antibiotic-resistant threats, leading to over 11,000 deaths per year in the U.S., alone [14]. Meanwhile, *E. faecium*, though not as abundant as *S. aureus*, accounts for 85% of all Enterococci species resistant to Vancomycin. Vancomycin-Resistant Enterococci (VRE) species are responsible for a variety of illnesses ranging from bloodstream infections to urinary tract infections. They account for an estimated 66,000 infections in the U.S. each year, leading to a recorded 1,300 deaths [14]. As one can see by the statistics, VREs are not as deadly as *S. Aureus*;

however, they continue to cause problems in hospital settings by causing infections.

Reason behind resistance in *Enterococcus Faecium*

Like other VREs, *E. Faecium* continues to present a challenge for therapeutic drug design. The source of resistance was unknown until a collaborative effort between members from different Massachusetts hospitals. They performed a 22-year study, detailing *E. Faecium* behavior in the presence of various kinds of antibiotics [15]. From 1968 – 1988, the team collected isolates and observed 6% of isolates displaying resistance towards penicillin and ampicillin. When members collected isolates again from 1989 – 1990, they saw a significant increase in resistance to clinically unachievable concentrations. They also recorded a high level of resistance towards other antibiotics such as streptomycin, kanamycin, and gentamicin (See Figure 2).

TABLE 2. Prevalence of penicillin resistance and HLR to aminoglycosides in *E. faecium*[a]

Source	% Isolates with:			
	Penicillin resistance[c]	HLR to aminoglycosides[b]		
		Strepto-mycin	Kana-mycin	Genta-micin
Solomon Islands (n = 24)	0	0	0	0
MGH (1968–1988; n = 48)	6[d]	42[e]	29[f]	0[g]
MGH (1989–1990; n = 36)	78[d]	83[e]	89[f]	61[g]

[a] Values with the same letter are significantly different (P <0.001).
[b] MIC, ≥2,000 μg/ml.
[c] MIC, ≥128 μg/ml.

Figure 2: Observation of resistance from collected isolates (14)

This figure not only shows that these species are resistant towards antibiotics, but also

highlights the evolution of bacterial species in developing new resistance mechanisms. Later on, a protein analysis study was conducted revealing six penicillin binding proteins (PBPs) potentially responsible for the antibiotic resistance of *E. Faecium* [16]. Of the six PBPs, Penicillin Binding Protein 5 (PBP5) was the most abundant and displayed the lowest affinity for the antibiotic. This indicated PBP5 as the main PBP and a major contributor to multidrug resistance of *E. Faecium*.

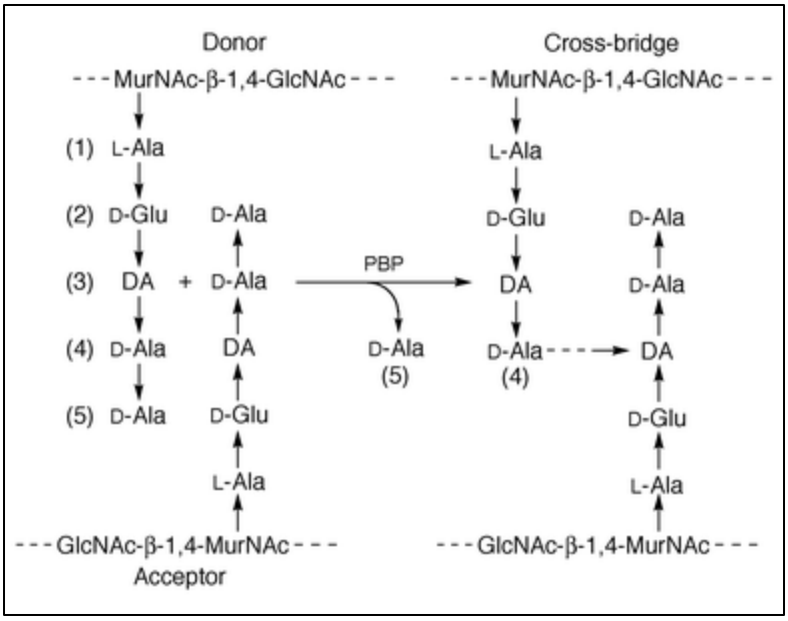

Figure 3: Cross-linking event leading to the exclusion of an Alanine Residue (F.1)

Penicillin Binding Proteins

Penicillin Binding Proteins (PBPs) are membrane bound proteins that play an essential role in the cell wall biogenesis function of specific bacterial species. They are members of a subgroup of enzymes known as transpeptidases, which are responsible for the cross-linking event that occurs between separate peptidoglycan chains, resulting in the formation of a rigid bacterial cell wall. Transpeptidation involves the identification of the D-alanine, D-alanine moiety [17] where a carbonyl group from the lateral amino residue of the acceptor glycan chain attacks the penultimate D-alanine from the donor glycan chain. This would result in the exclusion of the terminal alanine residue adjacent to the penultimate D-alanine from the donor glycan chain, marking the completion of the cross-link (Figure 3).

These cross-links between glycan chains give certain bacterial species the ability to

become resistant towards today's medical treatment. The current strategy for treating nonresistant bacterial species involves β-lactam antibiotics. These therapeutic drug substances are able to target the active site of PBPs and prevent their transpeptidase function from generating rigid bacterial cell walls. They are similar in chemical structure to the D-alanine, D-alanine moiety, in which case, PBPs "mistaken" them as the natural substrate during cell wall synthesis (See Figure 4). As a result, the antibiotic irreversibly reacts to the enzyme, forming an acyl enzyme complex that is unable to perform its transpeptidase function [18]. By inhibiting cell wall biosynthesis, cell walls decrease in strength and increase in permeability, causing in cytolysis and bacterial cell death [19].

In the case of resistance, PBPs will continue transpeptidase activity even when β-lactams are bound to their active site. Studies have shown how bacterial organisms from the *Streptococcus* and *Neisseira* genus can produce PBPs that are hardly affected by β-lactams [20,21]. In *Staphylococcus* species, methicillin resistance derives from the *mecA* gene, which is responsible for the production of PBP2a. Like many β-lactam resistant PBPs, PBP2a can easily orchestrate the assembly of new bacterial cell walls, even in the presence of high concentrations of antibiotics [22].

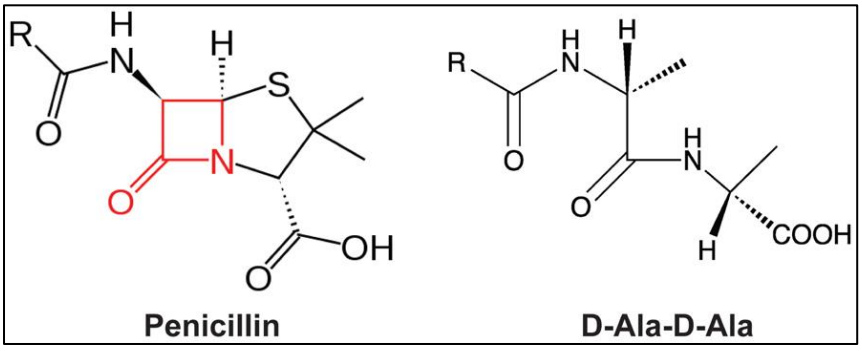

Figure 4: Chemical structure of Penicillin and the D-alanine, D-alanine moiety. The β-lactam ring is highlighted in red (F.2).

β-Lactam Antibiotics

β-Lactam antibiotics are a class of broad-spectrum antibiotics that act against a variety of bacteria causing diseases. As a broad-spectrum antibiotic, they work against both Gram-positive and Gram-negative bacteria. Gram-positive bacteria have a multilayered peptidoglycan layer and are more vulnerable to antibiotics compared to Gram-negative bacteria [23]. β-Lactams consist of a β-lactam ring within their chemical structure, which is a four-membered cyclic amide that is part of the core structure of several antibiotic families (See Figure 4). The name derives from the nitrogen atom being linked to a β-carbon relative to the carbonyl. The details of the structure were observed by the work from E.R. Squibb & Sons and the Florey group [24]. E.R. Squibb & Sons crystallized the penicillin compound from a United States strain while the Florey group crystallized it from an English strain. A comparison of the compounds revealed how English clinical trials used a 2-pentenylpenicllin (Penicillin F or I) derivative while the U.S. penicillin was benzylpenicillin (Penicillin G) [25]. Both substances revealed a commonality containing a β-lactam ring within their respective structures.

The biosynthesis pathway of the β-lactam core was discovered for that of penams and cephems. The pathway starts with the catalytic activity of ACV synthetase (ACVS), a nonribosomal peptide synthetase that produces ACV, a linear tripeptide. Then, an enzyme known as isopenicillin N synthase (IPNS) oxidatively cyclizes ACV to a bicyclic intermediate known as isopenicillin N. Cyclization is done twice by the same IPNS. The resulting penam structure will go through several stages of transamidation to generate a variety of natural penicillin products [26]*. The biosynthesis of cepham structures branch off from the formation of isopenicillin N through an oxidative ring expansion from the cephem core (See Figure 5).

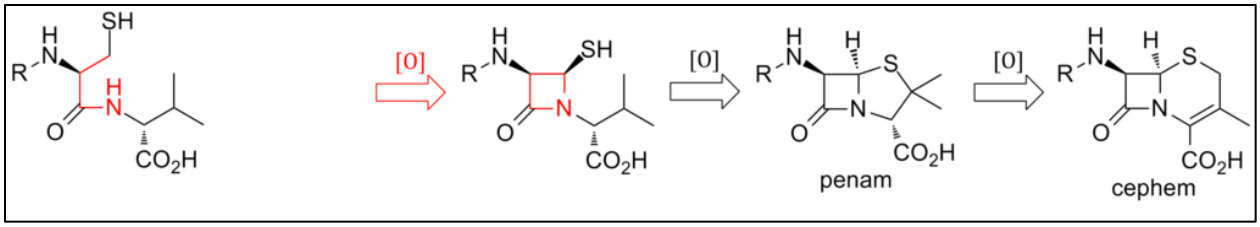

Figure 5: Outline of biosynthesis of penams and cephems (26).

Classification of PBPs

PBPs have been classified into two groups: high molecular mass (HMM) PBPs and low molecular mass (LMM) PBPs [27]. HMM PBPs are divided into two different classes depending on the structure and function of their N-terminal domain (Figure 6). Both Class A and Class B PBPs catalyze transpeptidation through the active site, which is located within the C-terminal domain. However, for Class A PBPs, the N-terminal domain comprises of a glycosyltransferase, which is responsible for elongating peptidoglycan chains that have yet to be involved in cross-linking events. They are known to be bifunctional PBPs where both domains of the enzyme complement one another, working together to build strong bacterial cell walls. Meanwhile, Class B PBPs are monofunctional PBPs where N-terminal domain activity remains unknown

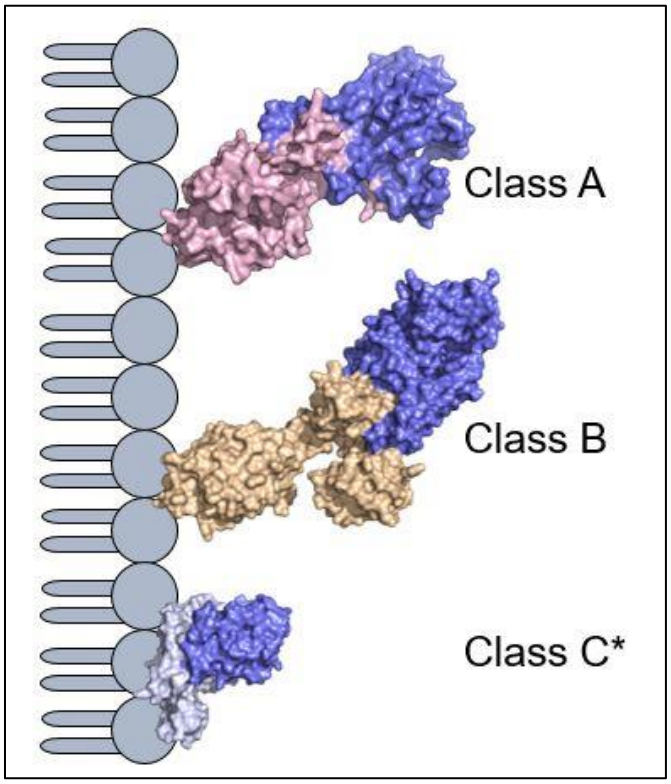

Figure 6: Class A PBP, represented by PBP2. Class B PBP, represented by PBP2a. Class C PBP, represented by PBP4. Transpeptidase domains are highlighted in blue. Class C* C-terminal domain function varies depending on type (F.3,F.4,F.5).

[28,29,30]. Since Class B PBPs lack glycosyltransferase activity, Class B PBPs must rely on other enzymes to provide them with elongated unchained strands for transpeptidase cross-linking. Class A PBPs were believed to be the main providers for Class B PBPs; however, recent findings have shown another transmembrane enzyme known as RodA to be the major supplier (See Figure 7) [31,32]. The basis for this prediction resided in two bacterial species, *Bacillius subtilis* and *Enterococcus faecalis*, who continued to survive in the absence of Class A PBPs. Another enzyme with glycosyltransferase activity must be at work, leading to the conclusion of RodA acting as the glycosyltransferase [33,34].

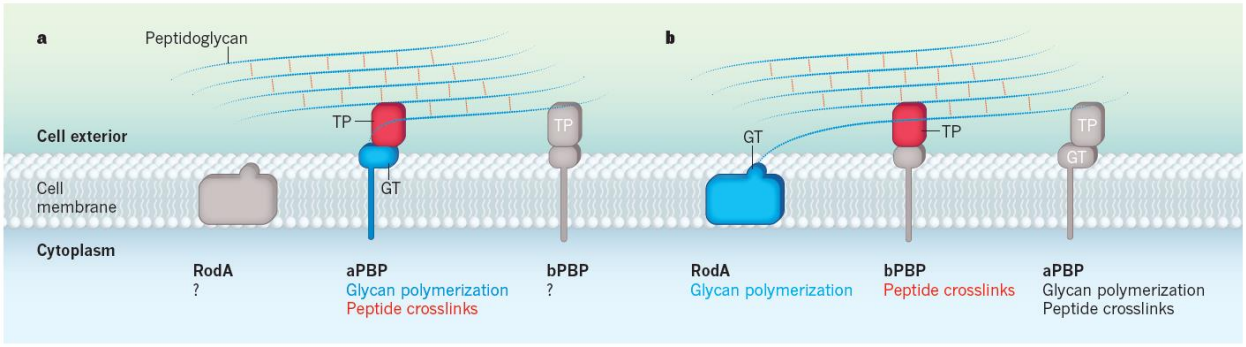

Figure 7: a. Displays normal Class A PBP activity. b. Proposed glycosyltransferase activity featuring RodA activity in conjunction with Class B PBPs (31,32).

LMM PBPs are generally classified as Class C PBPs with subdivisions depending on their activity. Not all Class C PBPs act as transpeptidases or glycosyltransferases. Type-4 and type-7 Class C PBPs act as endopeptidases, which perform the opposite function of transpeptidases by cleaving the peptide bonds that link glycan chains together [35]. Type -5 Class C PBPs act as carboxypeptidases, cleaving the terminal D-alanine, D-alanine bond on glycan strands, resulting in their unavailability for transpeptidation [36].

The Active Site

The active site of PBPs is largely conserved between the two classes of HMM PBPs. It lies between a domain consisting of a five stranded β-sheet sheltered by α-helices and another domain that is predominantly helical. Both domains are subdomains that make up the Penicillin Binding Domain where antibiotic binding takes place. Superposition of a Class A PBP with a Class B PBP shows conservation of the active site as well as important residues involved in penicillin binding. The active site is composed of three different motifs, where seven residues are strictly conserved amongst PBPs. The first motif, S*xxK, contains the active serine involved in acylation of the antibiotic and is positioned on an α-helix. The second motif, SxN, is located on a loop between two α-helices. Finally, the third motif, KTGx, is situated along a β-sheet (See Figure 8).

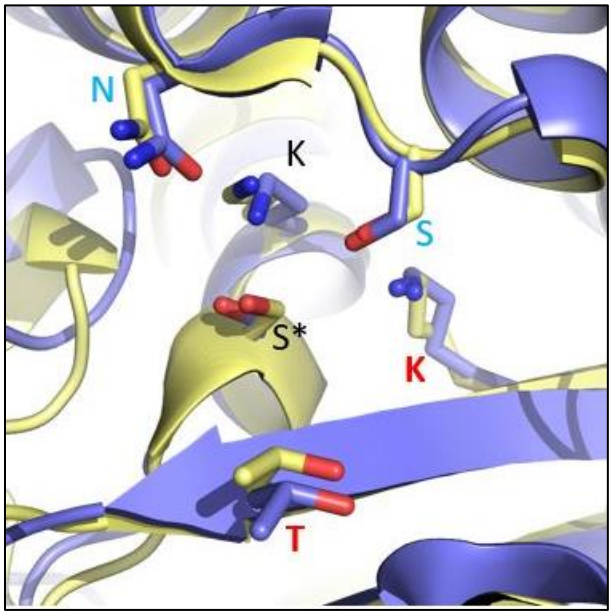

Figure 8: Overlay of active site of Class A PBP, PBP2 and Class B PBP, PBP2a, represented in cartoon format. Active site motifs are represented in sticks. SxxK motif in Black. SxN motif in Cyan. And KTGx motif in red (F.4, F.6).

Active Site Motif Interaction

All three motifs play a significant role in the positioning of the natural substrate to the active site. First, the active site serine from the first motif becomes deprotonated by the lysine residue from the same motif [37]. Acting as a nucleophile, the negatively charged serine will attack the penultimate alanine residue of the donor glycan strand, which acts as the electrophile. After electron shifting, the negatively charged natural substrate will become stabilized by

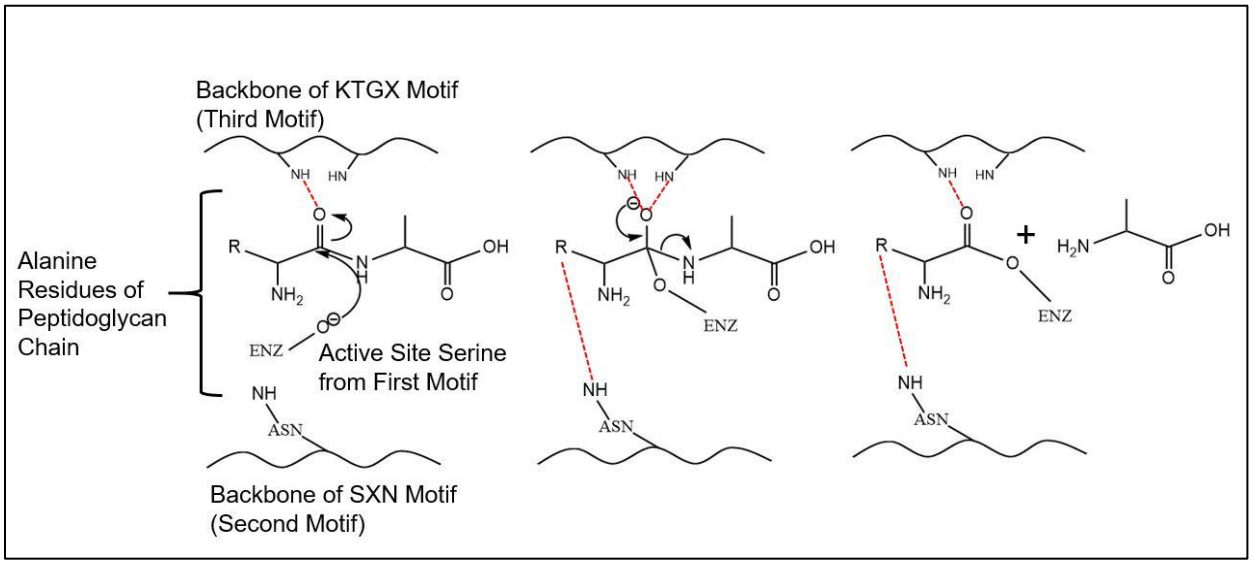

Figure 9: Curved arrow mechanism of motif interaction with the natural substrate (7)

backbone amine groups of the third motif, forming an oxyanion hole. Finally, the terminal alanine residue will become excluded from the natural substrate, marking the completion of the first step of transpeptidation (See Figure 9).

The next step involves cross-linking with the acceptor glycan strand and deacylation of the linked pair from the enzyme. This binding event will begin once an amino group of the acceptor strand becomes an activated group after deprotonation, which will attack the acyl-enzyme complex through carbonyl carbon from the ester bond [38,39]. Deprotonation can be performed by the lysine residue of the third motif or from the serine residue from the second motif with the help of the lysine of the third motif [40]. Based on the observed amino acid residue interaction, the active site can be thought of as a double lysine—serine system for both acylation and deacylation of peptide glycan strands.

Analysis of the structure of the acyl-enzyme complex shows specificity of the positioning of the natural substrate within the active site. Figure 10a displays the structure of PBP4a, a Class C PBP from *B. subtilis,* bound with a peptidoglycan mimic known as α-aminopiemlyl-ε-D-

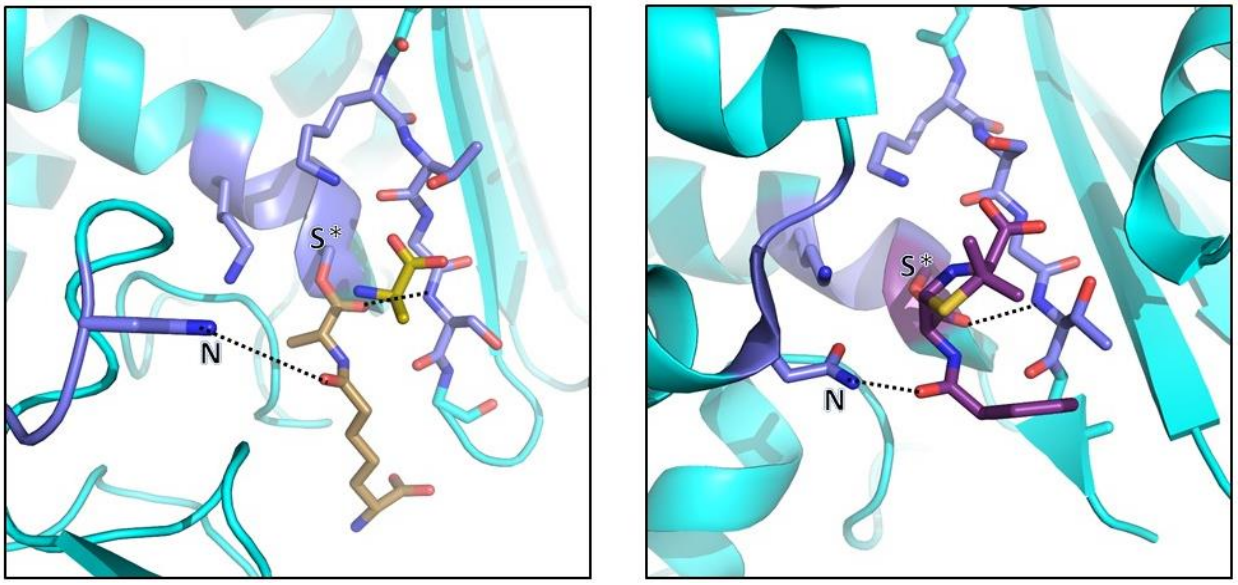

Figure 10: a) Structure of PBP4a with a peptide mimic. b) PBP2a with β-lactam (F.4, F.7).

alanyl-D-alanine. The unbound alanine within the structure marks the completion of the acylation reaction, as shown in Figure 9. The penultimate alanine residue of the donor glycan strand fitting tightly within the active site by a covalent bond with the active site serine from the first motif. Amide groups from the mimic are wedged between the asparagine residue of the second motif and the backbone amine groups along the β strand of the third motif. The carbonyl oxygen from the penultimate alanine lies within the oxyanion hole while the carboxylate of the excluded alanine is positioned near hydroxyl group side chains of the third motif. These observations demonstrate how the asparagine residue of the second motif and the hydroxyl groups from the third motif are imperative for precise positioning of peptide glycan chains to the enzyme [41].

β-lactam antibiotics are perfect inhibitors for these enzymes because of their ability to orchestrate a similar geometric position to the active site as their natural substrate. As seen in Figure 10b, the active site serine from the first motif breaks up the β-lactam ring of the antibiotic to form an irreversible covalent bond. The amide group of the side chain of the antibiotic is

enclosed within the space between the asparagine residue of the second motif and the backbone β-strand of the third motif. Hydroxyl groups of the third motif form hydrogen bonds with the carboxylate connected to the dihydrothiazine ring of the antibiotic. Similar interactions are portrayed with the excluded alanine residue as well. The carbonyl oxygen of the antibiotic also resides within the oxyanion hole, parallel to the carbonyl oxygen of the penultimate alanine of the natural substrate lying within the same area.

Acquired Resistance in PBP2a and PBP5

In Figure 10b, the structure displayed binding of Penicillin G to the active site of PBP2a from *S. aureus*. Despite irreversible acylation of the antibiotic, PBP2a successfully continues transpeptidation, completing bacterial cell walls during MRSA infections. Just as how PBPs can "mistake" the D-alanine, D-alanine moiety for β-lactam antibiotics, the reverse may also be true. For PBPs with a resistance mechanism like PBP2a, these enzymes may "mistake" the β-lactam antibiotic as a natural substrate, deacylating the antibiotic upon the arrival of another pair of unlinked glycan strands awaiting transpeptidation. Per Otero and his team, this resistance mechanism may also occur in PBP5 from *E. faecium* [42]. PBP5 could potentially have equivalents for Lobes 2 and 3 and the presence of a Lobe 1, as seen in the crystal structure of the PBP2a complex (Figure 11). Therefore, similar structural features could lead to similar resistance mechanism against β-lactam antibiotics.

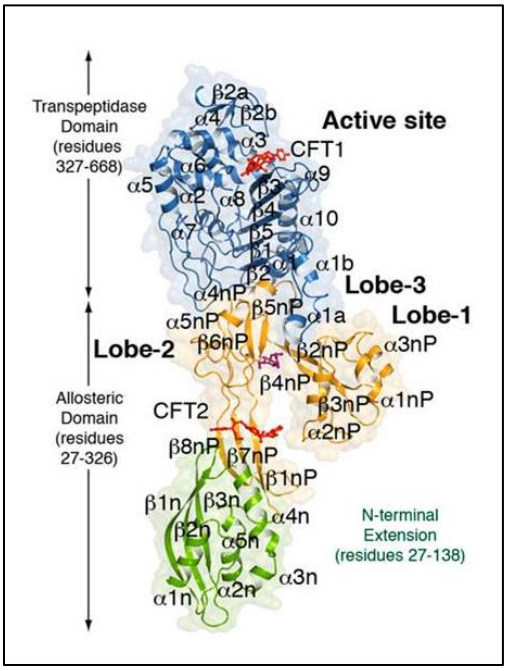

Figure 11: Crystal Structure of PBP2a in complex with two Ceftaroline molecules (42).

Methods

Protein Sample Preparation

Preparing PBP5 for analysis encompassed a number of stages:

1. Generation of Vectors

RP1B vectors of His-Tagged PBP5 enzymes without their membrane binding domains, had already been prepared by the Peti lab for the purpose of this study.

2. Generation of cell pellets

After sequencing RP1B vector samples to observe the desired protein sequence, they were then introduced into expression competent cells. BL21(DE3) cells (Invitrogen) containing expression plasmids were grown at 37°C in LB medium supplemented with appropriate antibiotics to an optical density (OD_{600}) of 0.8. Isopropyl β-D-1-thiogalactopyranoside (IPTG) was added to a final concentration of 0.5 mM and the cultures were incubated for an additional 18 hours at 18°C before being harvested by centrifugation. Pellets were stored at -80°C for later use.

3. Protein Purification

Pellets were suspended in lysis buffer (500 mM NaCl, 50 mM Tris pH 8.0, 0.1% Triton X-100, 5 mM Imidazole) containing EDTA-free protease inhibitor tablets (Roche Diagnostics) and lysed by high pressure homogenization using an Avestin C3 Homogenizer. Cell debris was removed by centrifugation at 50,000 x *g* for 50 minutes at 4°C, filtered through 0.22 μm polyethersulfone (PES) membrane filter (Millipore) and then loaded onto a HisTrap HP column (GE Healthcare) pre-equilibrated in Buffer A (500 mM NaCl, 50 mM Tris pH 8.0, 5 mM imidazole) for affinity

purification using the ÄKTA Prime Plus system (GE Healthcare). Bound protein was eluted on a linear gradient towards Buffer B (500 mM NaCl, 50 mM Tris pH 8.0, 500 mM imidazole). His_6-TEV-PBP5 eluted between 13 – 56% B. Fractions were pooled and dialyzed into 500 mM NaCl, Tris 50 mM at 4°C for 48 hours in the presence of TEV protease for protein cleavage. Following dialysis and protein cleavage, PBP5 was subtracted from free hexahistidine tag and TEV protease via gravity column loaded with Ni^{2+}-NTA agarose beads. TEV protease activity was confirmed through SDS gel. The flow-through, which contained the cleaved PBP5, was pooled and dialyzed for 2 hours at 20°C into 1.5 M $(NH_4)_2SO_4$, 10 mM Tris pH 8 in preparation for hydrophobic interaction chromatography. Dialyzed samples were loaded onto a HiTrap PhenylHP column (GE Healthcare) pre-equilibrated in Buffer A (1.5 M $(NH_4)_2SO_4$, 10 mM Tris pH 8) via ÄKTA FPLC system. PBP5 was eluted between 15 – 42%B, using a linear gradient towards 10 mM Tris, pH 8. Fractions were pooled and dialyzed into 800 mM NaCl, 10 mM Tris pH 8 at 20°C for 2 hours. PBP5 was concentrated and purified further by size exclusion chromatography loading onto a Superdex 200 26/60 column (GE Healthcare) pre-equilibrated in 800 mM NaCl, 10 mM Tris pH 8 by the ÄKTA Pure System. PBP5 was pooled, concentrated, and used for crystallization experiments. Protein purity was confirmed via SDS gel.

Protein Crystallography

PBP5 crystallization was tested with multiple concentrations ranging from 7 mg/ml to 60 mg/ml. Multiple crystal trays were produced for sitting drop vapor diffusion using the Art Robbins Phoenix. Completed trays were sealed by clear tape. Trays were both refrigerated at 4°C and placed at room temperature. Trays were periodically checked on days 1, 3, 7, 14, 21, 28, 31. After an optimal condition was found, crystals of apo PBP5 were reproduced at room

temperature using hanging drop vapor diffusion in 2.0 M Ammonium Sulfate, 0.1 M Tri-sodium citrate pH 5.5. To generate acylated complexes, we soaked crystals with ceftriaxone and imipenem in a 1:1000 molar ratio and 1:20 molar ratio, respectively for 1 hour. To generate PBP5:Penicillin G crystals, PBP5 was first incubated with Penicillin G at a 1:10 molar ratio for 1 hour before crystallization using hanging drop vapor diffusion in the same condition that resulted in apo PBP5 crystals. PBP5 and PBP5:Penicillin G crystals were cryoprotected in 5.0 M Ammonium sulfate while PBP5:Ceftriaxone and PBP5:Imipenem were cryoprotected in 4.5 M Ammonium sulfate.

Structural Analysis

X-ray data was collected in house using Rigaku FR-E+ Superbright rotating copper anode X-ray generator with Saturn 944+ HG detector (Brown University Structural Biology Facility). The initial models were built using Phenix AutoBuild followed by rounds of refinement in PHENIX and manual building using Coot. Molecular interactions were observed and analyzed through Pymol.

Results

1.1 The Structure of PBP5

The crystal structure of PBP5 was solved at 2.7 Å using data collected from crystals grown in conditions containing an acidic pH and high ammonium sulfate concentration. These crystals were optimized by fine screen, resulting in large, single rod-shaped crystals. Data analysis indicates the space group to be $P6_322$ with cell dimensions of a= 190Å, b= 190Å, c= 156Å, α,β=90, ɣ=120. The data was phased using molecular replacement (Phaser as implemented in PHENIX) using PBP2' (PDBID:5DVY) as the search model. The structure was refined against the collected data set with an R_{work} of 18% and an R_{free} of 21%. The final model contained 637 amino acid residues. The structure displayed two separate domains within the enzyme (Figure 12a) which are representative of an N-terminal domain and a transpeptidase like C-terminal domain seen in all HMM PBPs.

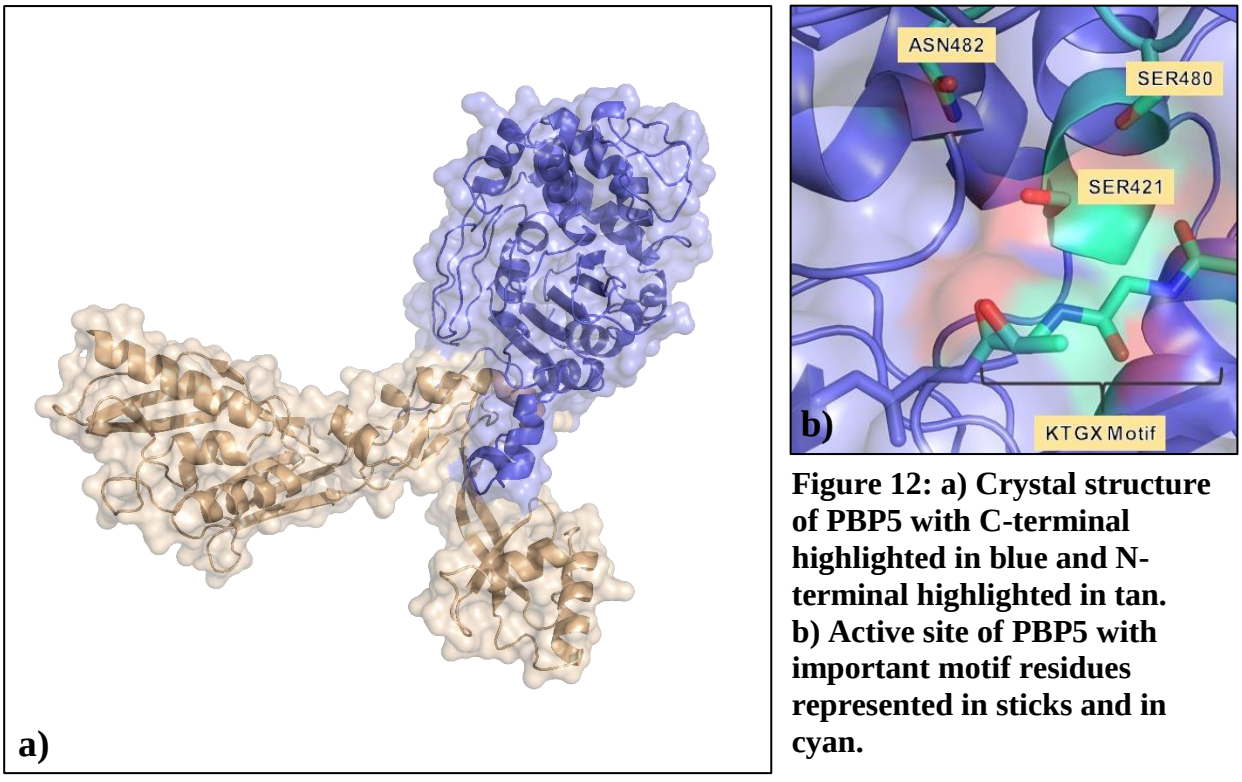

Figure 12: a) Crystal structure of PBP5 with C-terminal highlighted in blue and N-terminal highlighted in tan. b) Active site of PBP5 with important motif residues represented in sticks and in cyan.

The structure of PBP5 continues to show evidence of belonging in to the Class B PBP category as it shares the same five motifs found in all Class B HMM PBPs. Per the work of Goffin and his team, the sequence motifs this class commonly shares include: “Motif I: Arg-Gly-Xaa-Xaa-Xaa-Asp-Arg-Asn-Gly, Motif II: Arg-Xaa-Tyr-Pro-Xaa-Gly, Motif III: Gly-Xaa-Xaa-Gly-Xaa-Glu, Motif IV: Gly-Xaa-Asp-Xaa-Xaa-Xaa-Thr-Xaa-Asp-Xaa-Xaa-Xaa-Glu and Motif V: Thr-Gly-Asp(Glu)-Xaa-Leu-Ala-Xaa-Xaa-Xaa-Xaa-Pro-Ser-Xaa-Asp (39).” These motifs are generally located along the interface between the N-terminal domain and the C-terminal domain as seen in Figure 13.

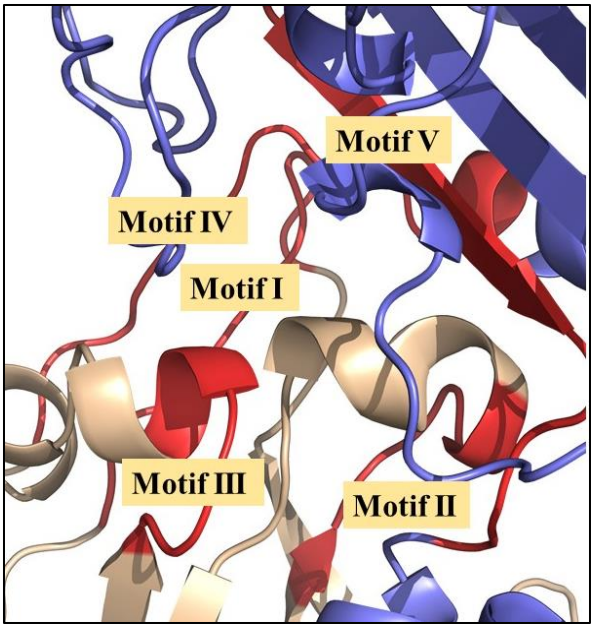

Figure 13: Motifs I-V that are found in all Class B PBPs represented in cartoon and in red.

1.2 Observable Penicillin Binding Site within PBP5

Structural analysis reveals three amino acid sequences that remain consistent with the three motifs that make up the general architecture of PBP active sites (Figure 12b). The first motif, the S*xxK motif containing the active site serine, is represented by Serine 421. This residue will play an important role during transpeptidation of the natural substrate or acylation of the β-lactam antibiotic. The second motif, the SxN motif, begins at Serine 480 and ends at Asparagine 482. These residues will naturally form hydrogen bonds with the substrate. The final motif, the KTGx motif, is represented by Lysine 616, Threonine 617, Glycine 618, and Threonine 619. The amide backbone of this motif will form an oxyanion hole with the substrate

to stabilize the transition energy during intermediate formation. These interactions displayed by these three motifs are observed in the structures of β-lactam acyl-enzyme complexes.

1.3 The Structures of β-lactam acyl-enzyme complexes

The crystal structures of PBP5:Penicillin G and PBP5:Imipenem were solved at 2.9 Å and 2.8 Å, respectively using data collected from crystals grown in conditions similar to those that grew PBP5 apo crystals. PBP5:Penicllin G crystals were grown by cocrystallization where the PBP5:Penicllin G protein solution was mixed at a 1:10 protein to antibiotic molar ratio. The mixture was incubated for 2 weeks before crystal formation via hanging drop diffusion. PBP5:Imipenem crystals were grown by soaking. PBP5 apo crystals were soaked with the antibiotic at a 1:10 and 1:20 protein to antibiotic molar ratio. After data collection and analysis, space group and cell dimensions of both structures remained the same as the PBP5 *apo* structure. The PBP5:Penicllin G structure was refined against the collected data set with an R_{work} of 19% and an R_{free} of 21%. The PBP5:Imipenem structure was refined against the collected data set with an R_{work} of 18% and an R_{free} of 22%. Both structures contained 637 amino acid residues with electron densities revealing a covalent acyl-enzyme bond between Serine 421 and each respective antibiotic (Figure 14).

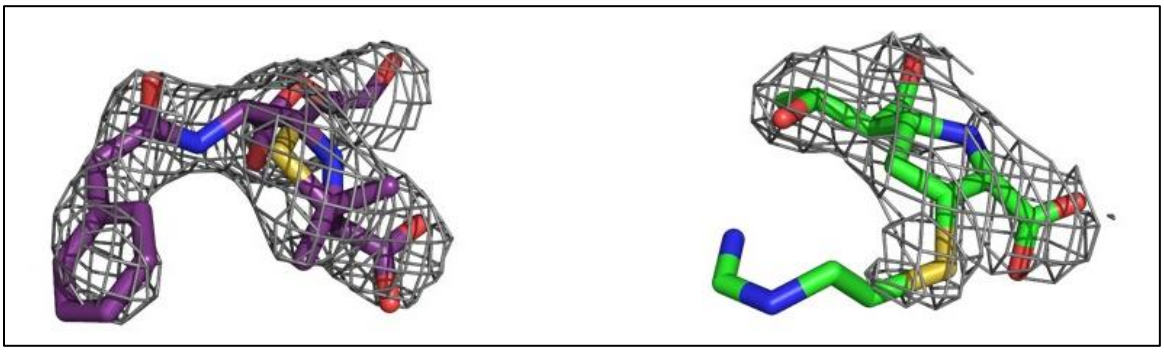

Figure 14: Electron density maps surrounding each respective antibiotic bound to PBP5 contoured at 1.0σ.

1.4 Comparing active site interactions with each respective β-lactam

After structural analysis, we observed how both β-lactam acyl-enzyme complexes share similarities in active site motif interaction. Firstly, the carboxylate oxygen from each respective antibiotic forms a hydrogen bond with Threonine 616 of the KTGx Motif. Bond lengths are almost identical between each β-lactam acyl-enzyme complex with the carboxylate oxygen on Penicillin G resting 2.7 Å from Threonine616 while the carboxylate oxygen on Imipenem rests 2.5 Å from the same residue. Secondly, the carboxamide nitrogen of Asparagine 482 of the second motif interacts with another carboxylate oxygen of each respective antibiotic. Bond lengths are almost identical for this case as well, with Penicillin G resting 2.8 Å away from the Asparagine residue and Imipenem resting 2.7 Å away from the same residue. Finally, the ring nitrogen of each antibiotic interacts with the hydroxyl side chain of Serine 480 of the SxN motif. The side chain was measured to be 2.9 Å from bound Penicillin G and 2.7 Å from bound Imipenem.

We were also able to observe differences between how each antibiotic interacts with PBP5. After comparing each respective β-lactam acyl-enzyme complex, one noticeable difference includes an insertion difference between the 2nd and 3rd motifs of the active site. In the PBP5:Penicillin G structure, only the amide side chain lies between the 2nd and 3rd motif. In the PBP5:Imipenem structure, both the imino-methyl-amino side chain as well as the hydroxyethyl side chain lies between the 2nd and 3rd motif. Another noticeable disparity involves the antibiotic geometric positioning within the oxyanion hole. For Penicillin G, the acyl linkage carbonyl oxygen lies within the oxyanion hole after acylation. In the case of the PBP5:Imipenem structure, the acyl linkage carbonyl oxygen lies far away from both the oxyanion hole and the KTGx motif

(Figure 15b). In summary, differences in antibiotic interaction with the active site were mainly attributed to differences in antibiotic chemical structure.

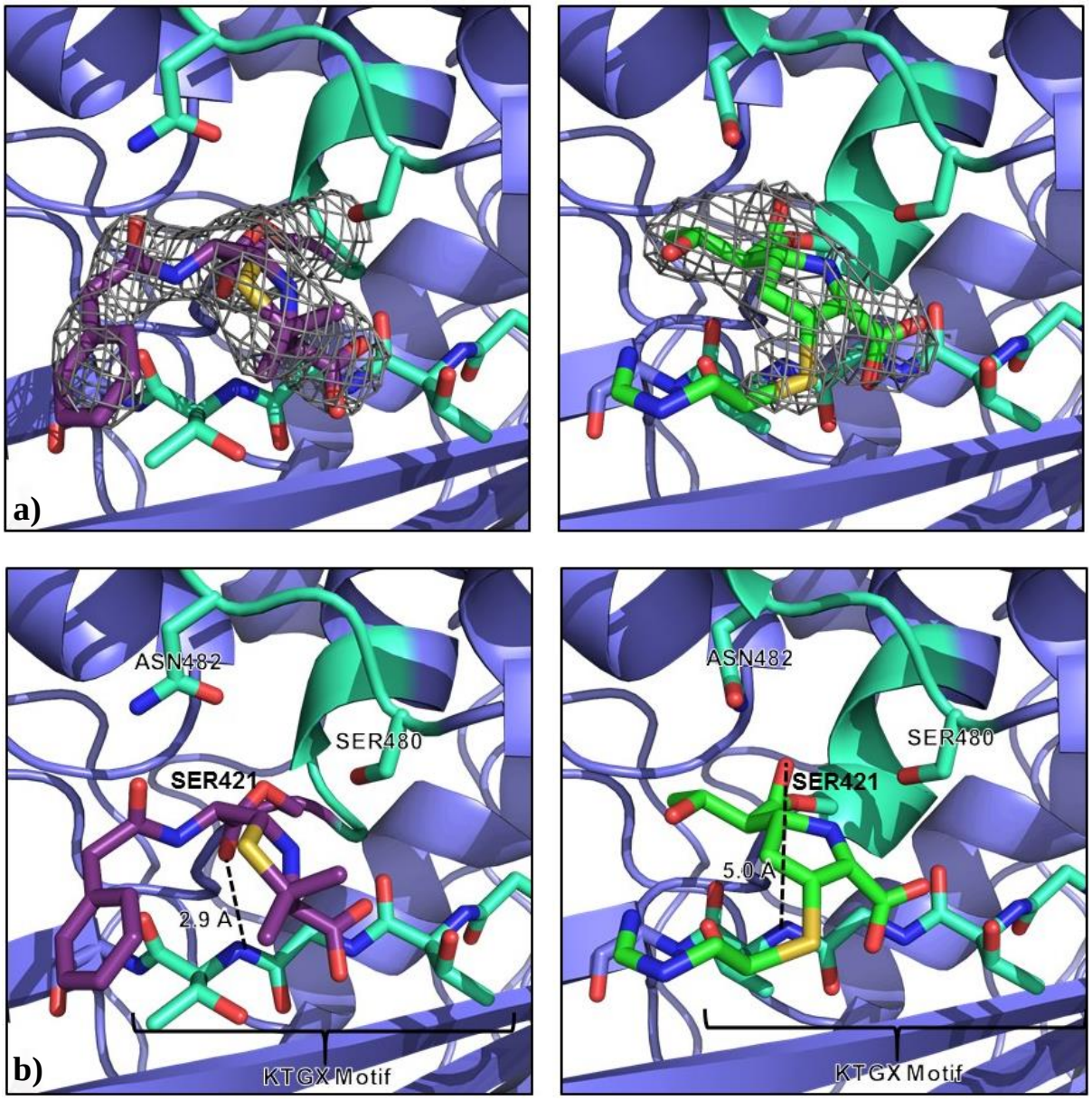

Figure 15 a) Electron density maps of each antibiotic within the active site of PBP5. b) Side by side contrast revealing differences in geometric positioning of Penicillin G within the active site and Imipenem within the active site of PBP5.

1.5 Absence of significant conformational changes after β-lactam acylation

To verify the conformational changes that result from acylation by β-lactam antibiotics, we compared our two acylated structures to that of our apo PBP5 structure. Superposition of the backbones of each respective structure reveal that all structural differences originate from the active site region of PBP5. Differences are dependent upon the chemical structure of each specific β-lactam and how they interact within the active site. RMSDs for the main chain atoms of the active site residues between acylated structures and apo structures range from 0.209 Å to 0.360 Å. Aside from the active site region, structural alignment of PBP5 apo, PBP5:Penicillin G, and PBP5:Imipenem reveal few disparities between the overall structure as seen in Figure 16. RMSDs for the main chain atoms of the amino acid residues of the whole structure between acylated structures and apo structures range from 0.215 Å to 0.227 Å.

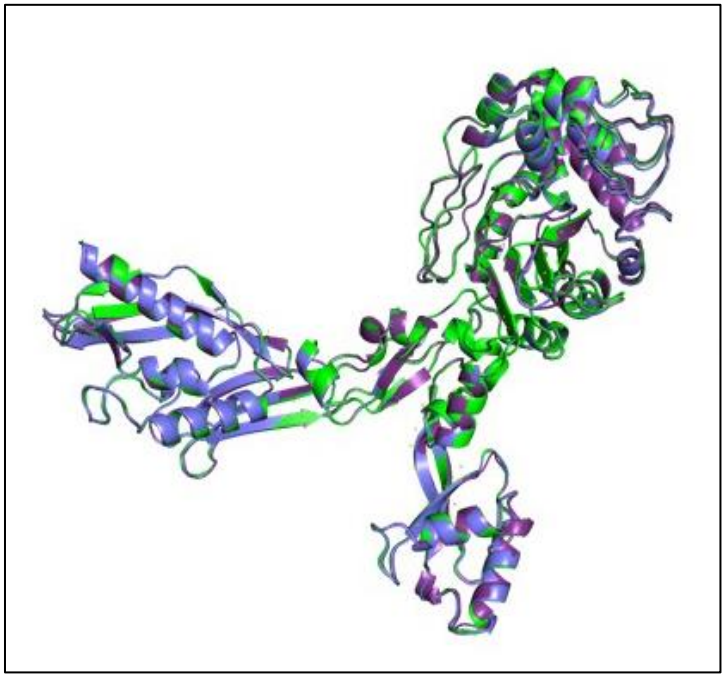

Figure 16: Structural overlay of PBP5 apo and β-lactam acyl enzyme complexes all represented in cartoon. PBP5 is represented in blue, PBP5:Penicillin G in purple, and PBP5:Imipenem in green.

2.1 PBP5 sequence comparison to PBP2a

Sequence Alignment of PBP5 and PBP2a from *Staphylococcus aureus* was done to determine amino acid conservation among these two Class B PBPs. Both enzyme sequences contained the five amino acid motifs that categorize them as Class B PBPs, which are

highlighted in red in Figure 17. Sequence alignment also revealed a high degree of variability in the overall structure with only 35% of residues being identical and 60% of residues being similar in chemical activity. Despite this variability between the structures, the active site remains highly conserved with 84% conservation. Complete conservation was unobtainable due to a difference in the amino acid residues of the third motif where a threonine in PBP5 is substituted for a serine in PBP2a.

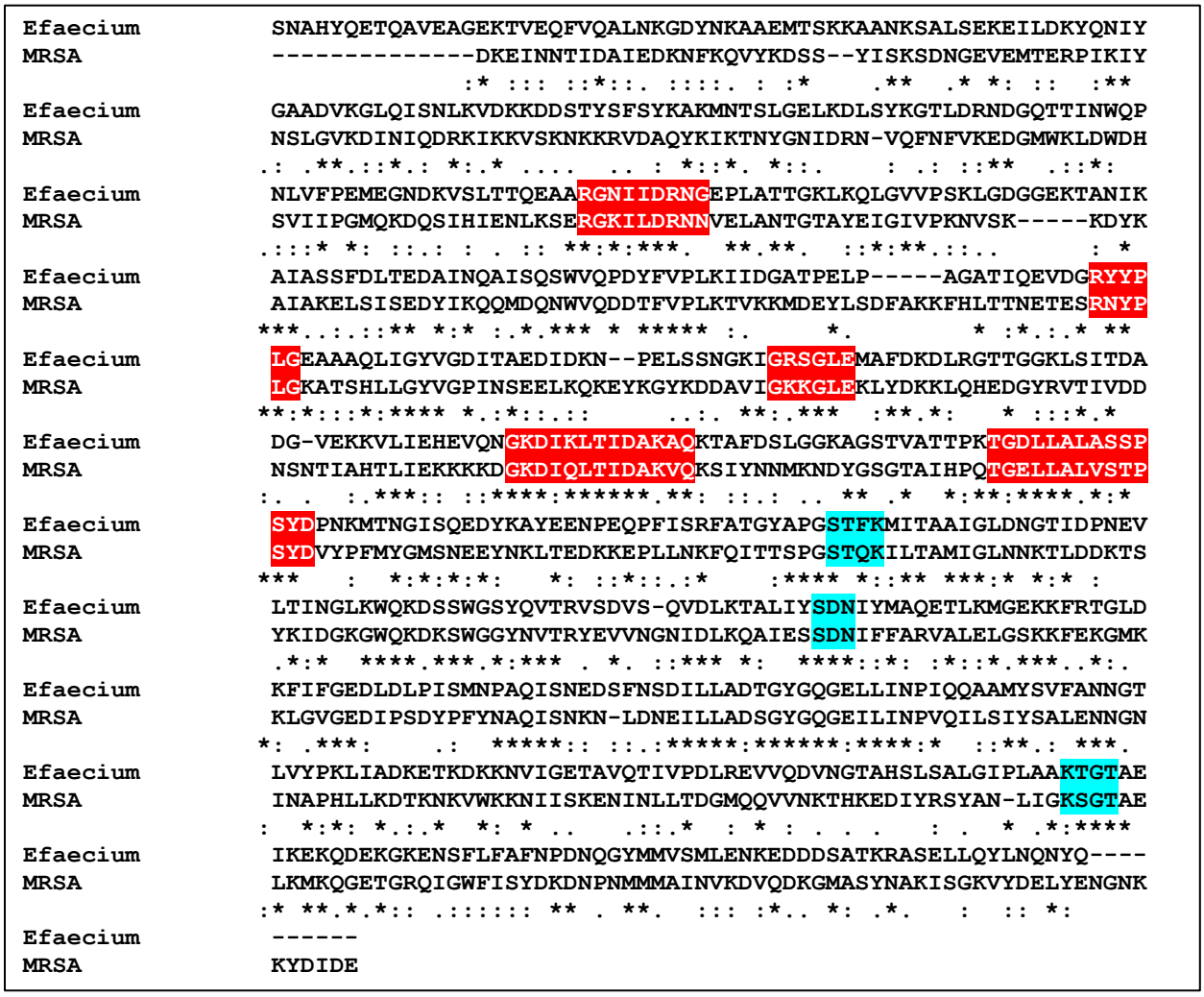

Figure 17: Sequence alignment of PBP5 (Efaecium) and PBP2a (MRSA). The 5 motifs found in all Class B PBPs are highlighted in red. The amino acid residues that make up the active site are highlighted in cyan.

2.2 Superposition of apo PBP5 structure and PBP2a

As expected, structural analysis reveals high variability between the overall structures. A large contribution to the resulting variability lies within inconsistencies along the N-terminal domain; however, this may be due to crystal packing differences between PBP5 and PBP2a. By contrast, the C-terminal domain demonstrated a larger conservation, specifically within the active site where RMSDs of the backbone amino acid residues of the active site ranged from 0.6 Å to 0.8 Å (Figure 18). As seen in the Figure 18, the natural geometric positioning of the three active site motifs of each PBP is very similar. As mentioned earlier, the main difference, aside from small bond angle contrasts, is the threonine residue in the third motif of the active site of PBP2a. Comparable positioning is reflective of how these enzymes interact with β-lactam antibiotics.

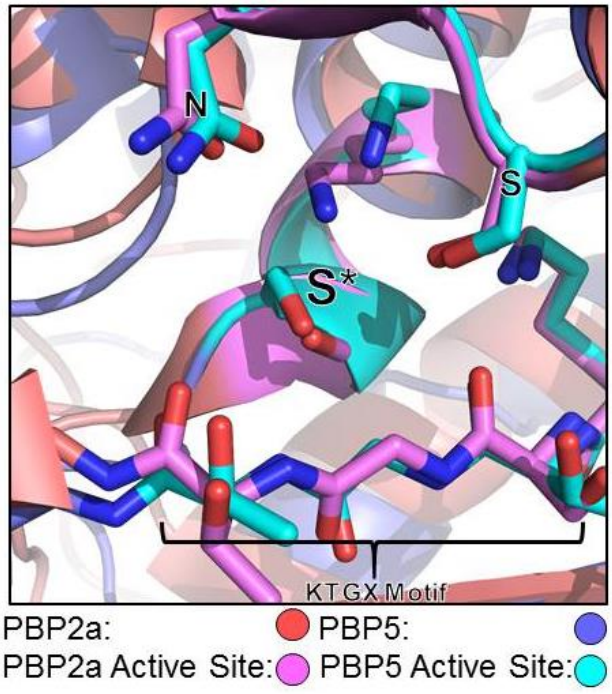

Figure 18: Structural analysis of PBP2a (red) and PBP5 (blue). Active site of both PBPs are represented in sticks with PBP2a Active Site residues in pink and PBP5 Active Site residues in cyan. (37)

2.3 Superposition of PBP5:Penicillin G and PBP2a:Penicillin G

The active site of each respective β-lactam acyl enzyme complex remains largely conserved with RMSDs ranging from 0.3 Å to 0.4 Å. Both display only minor differences in active site interaction with Penicillin G. Hydrogen bond networks between the antibiotic and the active site residues are very similar between both structures as well. Both structures showcase the carboxamide nitrogen of the asparagine residue of the second motif interacting with the carboxylate oxygen of the antibiotic. These interactions occur at similar bond lengths with PBP2a having the interaction occur at 2.7 Å and PBP5 having the interaction occur at 2.8 Å. Each structure also reveals how the serine residue of the second motif interacts with the ring nitrogen of Penicillin G. In PBP2a, the bond length is 3.2 Å while in PBP5, the bond length is 2.9 Å. Meanwhile, a carboxylate side chain on the Penicillin G molecule adjacent to the active site serine forms a hydrogen bond with the amide backbone of the third motif at 2.9 Å in both PBP2a and PBP5. This specific interaction leads to the mentioned formation of an oxyanion pocket to stabilize the substrate during intermediate formation (Figure 19).

Despite differences in the identity of the amino acid residue, with respect to the third motif of the active site, the serine of PBP2a and the threonine of PBP5 act in a similar fashion. Their contrasting identities may have contributed to the resulting RMSD range; however, we observed the carboxylate oxygen of each residue interacting with the carboxylate oxygen along the Penicillin G molecule. Both structures revealed interactions at similar bond lengths as well with the serine residue in PBP2a measuring at 2.6 Å and the threonine residue in PBP5 measuring at 2.7 Å (Figure 19). Aside from differences in residue identity, there was no other significant differences observed between PBP5 active site interaction with Penicillin G and PBP2a active site interaction with Penicillin G.

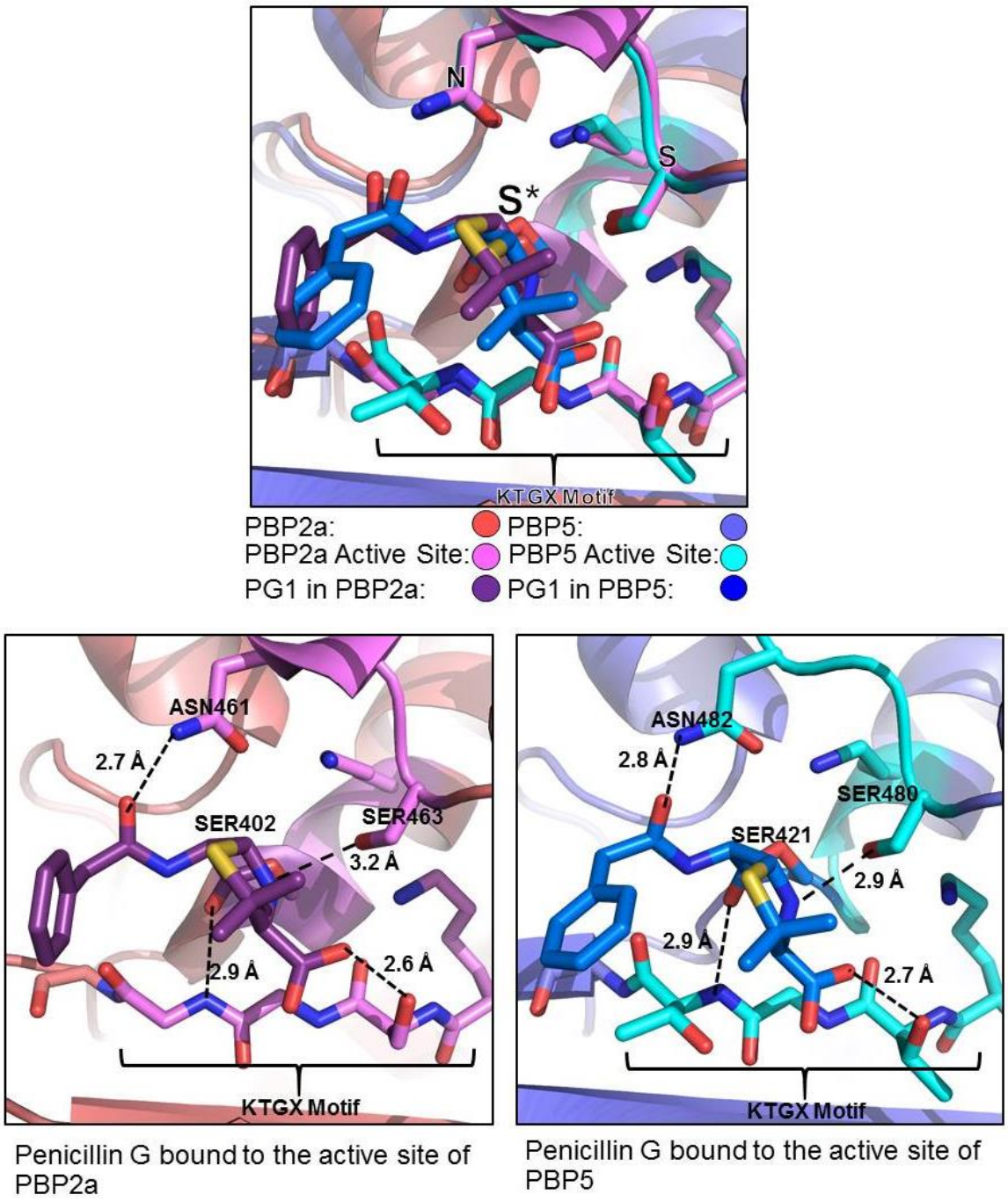

Figure 19: (Top) Structural overlay of PBP2a in complex with Penicillin G and PBP5 in complex with Penicillin G. Active site residues are represented in sticks as well as Penicillin G (Bottom left) Bond length measurements of motif interaction with Penicillin G in PBP2a (37). (Bottom right) Bond length measurements of motif interaction with Penicillin G in PBP5.

3.1 Allosteric Domain Comparison between PBP2a and PBP5

It was proposed by Otero and his team, that some Class B PBPs may house an allosteric domain within their structure. They suggest that the allosteric domain lies along the interface that connects the C-terminal and N-terminal domain as seen in Figure 20. The structure of the PBP2a complex solved at 2.6 Å reveals the usual acyl aduct in the active site of the C-terminal transpeptidase being occupied by a second generation β-lactam antibiotic known as Ceftaroline. Their structure also reveals a second Ceftaroline molecule within a region where they suggest is an allosteric site. They believe that this occupancy within the allosteric site plays a pivotal role in active site substrate binding. This hypothetical mechanism of inactivation of PBP2a catalytic activity has the potential to open many opportunities in future drug design strategies. Per Otero and his team, this unique mechanism may also be found in PBP5 from *E. faecium*, via a random event of natural selection, which resulted in a beneficial characteristic for the organism [43]. To determine whether this unique interaction takes place in PBP5, we investigated how PBP2a interacts with Ceftaroline.

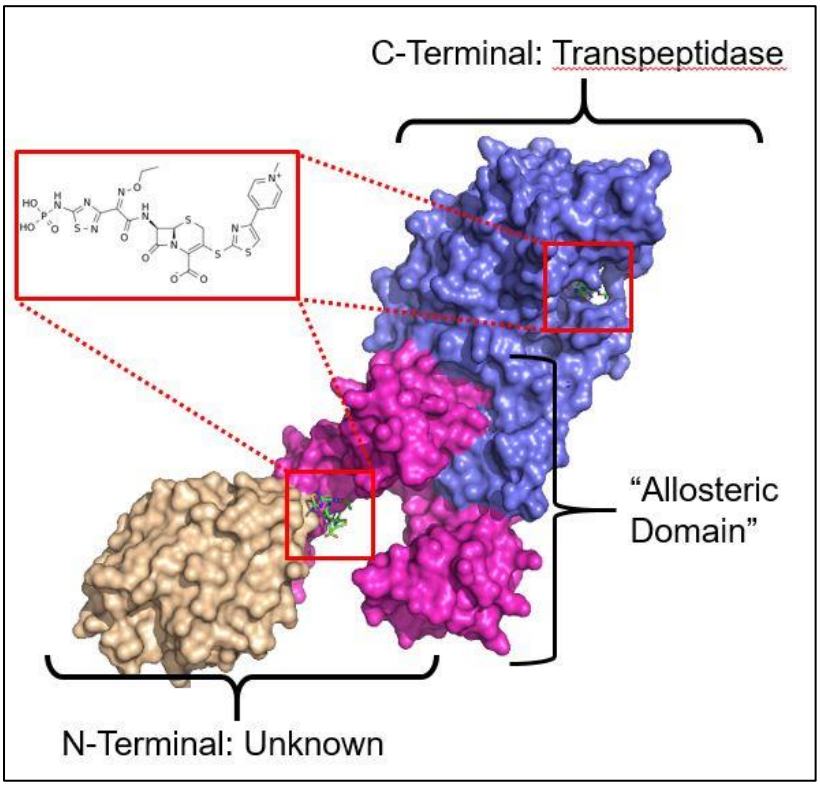

Figure 20: Structure of PBP2a. C-terminal in blue. N-terminal in tan. Proposed allosteric domain in magenta. Two ceftaroline molecules highlighted in green sticks (42)

3.2 PBP2a interaction with Ceftaroline

Otero and his team suggest noncovalent binding of a Ceftaroline molecule to their proposed allosteric site. Structural analysis depicts the β-lactam moiety of ceftaroline making several polar contacts with proximal tyrosine residue side chains. With respect to chemical structure of Ceftaroline as seen in Figure 21, the R1 group of the second generation β-lactam antibiotic also forms polar contacts with Asparagine 104 and Lysine 76. Meanwhile, the R2 group is entrapped in a pocket formed by Isoleucine 144 and Tyrosine 105. After noncovalent binding, it appears that unique salt bridge interactions are observed connecting the interface to the C-terminal transpeptidase domain. Unique salt bridge interactions occur around the Ceftaroline molecule within the allosteric region as well (Figure 22). Generally, most side chain interactions and the resulting minority of backbone interactions are standard in substrate to enzyme binding, as seen in the antibiotic binding to the PBP2a active site. However, as seen in Figure 22, backbone interactions are the majority and are being reported to interact heavily with Ceftaroline. Superposition of the structure with our β-lactam acyl enzyme complex of PBP5:Penicillin G will help further investigate the exclusivity of this binding mechanism.

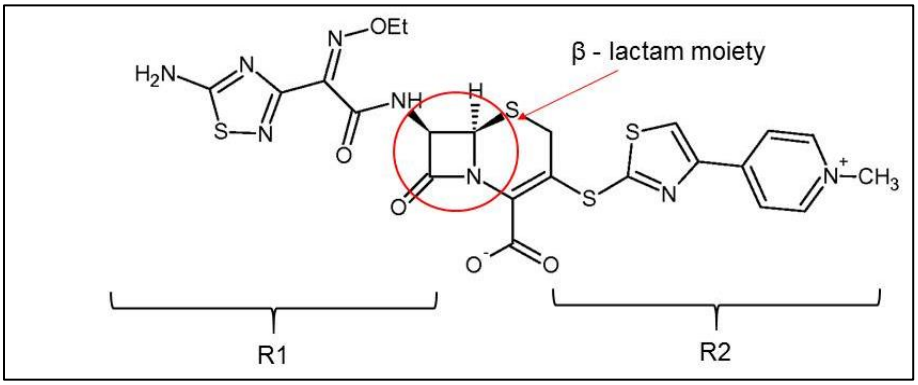

Figure 21: The chemical structure of Ceftaroline. β-lactam moiety is circled in red. R1 and R2 groups residing on each side of the β-lactam ring are labeled.

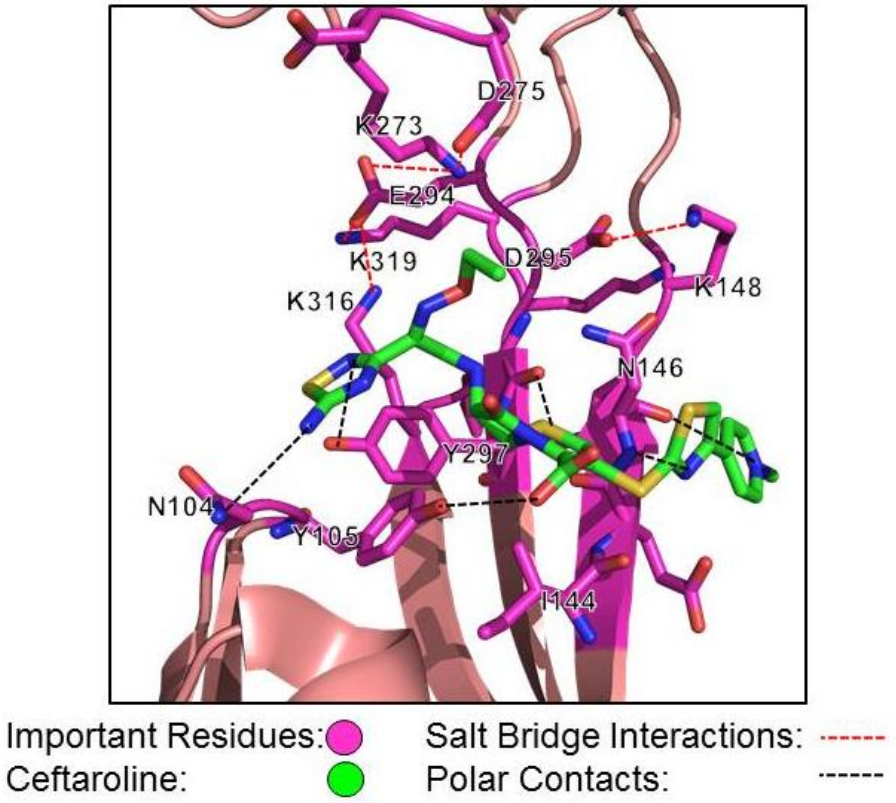

Figure 22: Salt bridge interactions within the proposed allosteric site are signified by red dashed lines while polar contacts are signified by black dashed lines (42).

3.3 No evidence of an allosteric region within PBP5

To determine the presence of an allosteric region within PBP5, we wanted to search for any conservation of amino acid residues that had the potential of forming salt bridges or polar contacts as seen by Otero and his team (Figure 23). After, Clustal Omega Sequence Alignment indicates no such conservation exists within the described region. PBP5 has no identical residues to those involved in the allosteric site of PBP2a. With respect to the residues involved in allosteric interaction in PBP2a, only 43% of residues in PBP5 act similarly. Superposition of the amino acid residues supposedly involved in the proposed allosteric region display a high level of variability between PBP2a and PBP5. After structural alignment of the residues involved in

allosteric binding in PBP2a and residues that have the potential to act similarly in PBP5, analysis indicates there is very little conservation observed within this region. The resulting RMSD value ranges from 2.7 Å to 2.9 Å. In addition, the residues that appear to be conserved do not align very well. Variability may be due to the crystallization process having a large effect upon the N-terminal domain making it difficult to observe a consistent overlay along the interface between the two domains of each respective complex. However, sequence alignment and structural alignment demonstrate that there is no current evidence of an allosteric region within PBP5.

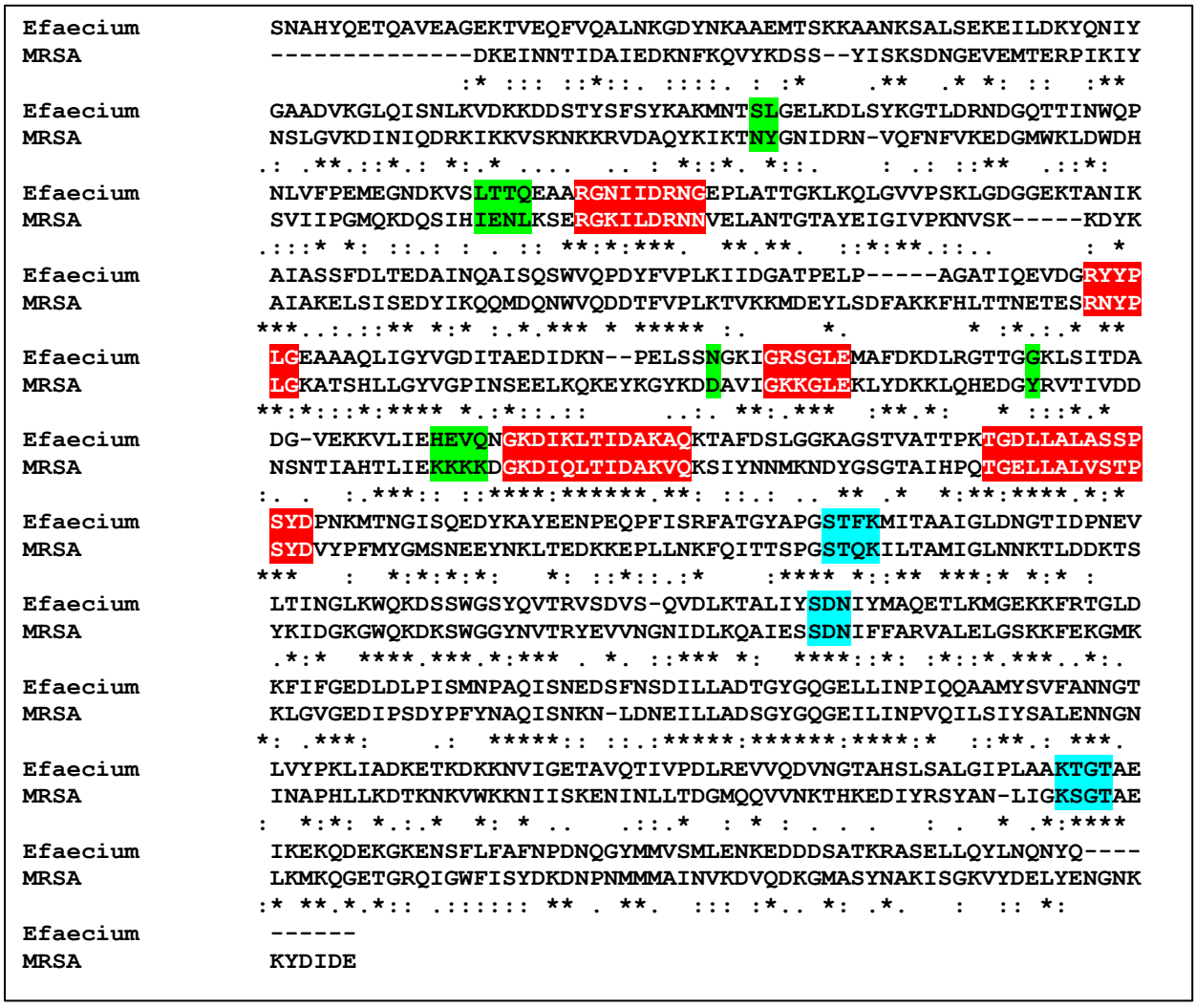

Figure 23: Sequence alignment of PBP5 and PBP2a. Allosteric residue in PBP2a and potentially similar residues in PBP5 are highlighted in Green.

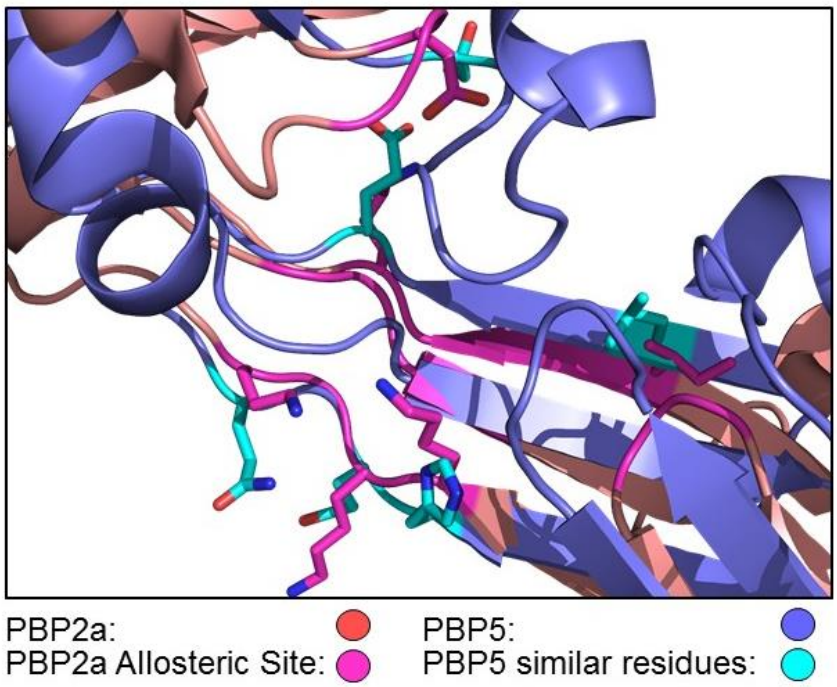

Figure 24: Important residues involved in allosteric binding are represented in stick formation. Similar residues in PBP5 are also represented in sticks.

Discussion

To determine how PBP5 in *Enterococcus faecium* interacts with different antibiotics, various crystals were produced under a wide variety of conditions. Pure protein at a concentration of 15 mg/ml was screened against many commercially available crystal screens with optimal crystals emerging from conditions containing a high ammonium sulfate concentrations and an acidic pH. This condition was then used to produce crystals of the following enzyme complexes: PBP5:Penicillin G, PBP5:Imipenem, and PBP5:Ceftriaxone. Different methods of crystal production such as cocrystallization and soaking were performed, resulting in optimal crystals that generated diffraction data sufficient for modeling the PBP5:Penicillin G and PBP5:Imipenem structures. Determining the structure of PBP5:Ceftriaxone introduced a challenge for us as Ceftriaxone was part of a drug class different from Penicillin G and Imipenem. As a prodrug, Ceftriaxone is manufactured as an inactive substance and will become active once the drug is metabolized or goes through a specific chemical reaction (Supplemental Data).

What this chemical reaction entails in regards to Ceftriaxone is an electron shift leading towards a leaving group once the active form of the drug is bound to the active site of PBP5. Therefore, unaccountability for this prodrug activity could lead to partial binding between Ceftriaxone and PBP5. As opposed to complete binding, partially bound samples may affect the crystallization process. This was verified through Mass Spectrometry (Supplemental Data) where a 1:10 and a 1:100 PBP5 to Ceftriaxone molar ratio were shown to be insufficient to produce complete binding for complex formation. Instead, a 1:1000 PBP5 to Ceftriaxone molar ratio produced complete binding, which was then followed by a second Size Exclusion Chromatography step to separate our enzyme complex from the sulfate leaving groups. This

complex was immediately screened against our personally designed Ammonium Sulfate Grid Screen where we were able to produce multiple PBP5:Ceftriaxone crystals. Much to our surprise, these crystals grew at a specific ammonium sulfate concentration and at a basic pH instead of acidic. Unfortunately, these crystals produced poor diffraction data and further optimization and investigation is necessary. Ammonium sulfate concentrations above 2.6 M seem to be the preferred salt condition for these crystals; however, the buffer for basic pH was variable. Crystals emerged from a variety of buffers including MES, HEPES, Tris, and BICINE at a pH range between 6.0 to 9.0. More crystal trials would need to be conducted to pinpoint the best condition for growing a PBP5:Ceftriaxone crystal.

Overview of the structural alignments of our apo PBP5 structure with respective β-lactam acyl enzyme complexes reveal little to no conformational change after antibiotic acylation in the active site. Differences between β-lactam acyl enzyme complexes are mainly due to differences in the chemical structure of each respective antibiotic. Superposition of the apo PBP5 structure with each complex showcases the ineffectiveness of antibiotics on PBP5. This potentially could give reason as to why *Enterococcus faecium* is resistant towards current antibiotics. Further analysis of the structures implies a previously proposed resistance mechanism where PBP5 could "mistaken" a bound β-lactam antibiotic for a natural substrate. Acylation of the antibiotic can be followed up with deacylation, possibly due to an acquired mutation where PBP5 recognizes the antibiotic as a cross-linked glycan chain. This would result in an opening for another peptidoglycan strand cross-linking event; and thus, continue catalytic function of transpeptidation. This resistance mechanism would explain how clinical isolates of *Enterococcus faecium* continued to function under moderate to high concentrations of various types of antibiotics such as ampicillin and ceftriaxone [44]. Arbeloa and her team observed resistance as

an intrinsic property, and that acquisition of high-level resistance was due to the ability of the bacterial species to overproduce PBP5 [45, 46, 47]. Further studies should be done such as taking ITC measurements, to obtain data regarding the bond strength between PBP5 and the antibiotic as well as PBP5 with a possible peptide mimic. This may help give evidence to support the proposed resistance mechanism.

This mechanism of misrecognition is also believed to be observed in PBP2a from *Staphylococcus aureus* [43]. Comparing the active site structure of PBP5 with PBP2a, we saw many similarities in the geometric positioning of important amino acid residues, indicating conservation of the active site. We also saw similarities in their respective active site interactions with antibiotics, revealing bond lengths and hydrogen bonding networks to be almost identical. The main disparity between PBP5 and PBP2a revolved around the subject of the existence of an allosteric region within PBP5. Otero and his team reported an allosteric domain located along the interface connecting the C-terminal and N-terminal domains of PBP2a. However, further analysis revealed the questionable geometry within the reported polar contact network and hydrogen bond network. Backbone interactions are being reported to be the main point of contact with the Ceftaroline molecule, which is a rare occurrence in binding sites. Nonetheless, sequence alignment and structural analysis designate high variability of this proposed region within the structure of PBP5. Therefore, there is no current evidence of an allosteric site within PBP5. Further crystallography studies followed by structural analysis should be done to help determine the absence of an allosteric domain within PBP5 from *Enterococcus faecium.*

Conclusion

Antibiotic resistance has become a major roadblock in modern medical treatment. It has the potential to bring forth the "post-antibiotic era" where bacterial infections could, once again, lead to inevitable death. Bacterial species continue to evolve and develop new resistance mechanisms that make current antibiotics ineffective. Luckily, appropriate steps are being taken by the CDC, WHO, and the United Nations to prevent the arrival of the "post-antibiotic era". Such measures led to minor discoveries that made large contributions into novel antibiotic drug design. For example, clinical isolate studies displayed how some bacterial species are resistant towards antibiotics due to PBP overproduction and activity. By recognizing PBPs as the major player in antibiotic resistance, structural analysis of the protein would be needed to provide additional information on how these proteins interact with current antibiotics.

Therefore, the collected data on the Class B PBP, PBP5 from *Enterococcus faecium* has the potential to be beneficial in future drug design strategies for inhibiting PBP transpeptidase function. We demonstrated how PBP5 can be expressed, purified, and crystallized to produce sufficient diffraction data for modeling and structural analysis. The provided structure of PBP5 as well as β-lactam acyl enzyme complexes PBP5:Penicillin G and PBP5:Imipenem help further our understanding on how this enzyme interacts with today's antibiotics. Structural comparisons between the apo structure and the complex structure as well as comparisons with other Class B PBPs such as PBP2a and PBP2a in complex with Penicillin G, imply a conventional resistance mechanism, which can be useful when creating innovative medical treatments for transpeptidase inhibition. Thus, our PBP5 structural studies may be a small yet important contribution to prevent the arrival of a "post-antibiotic era".

Supplemental Data

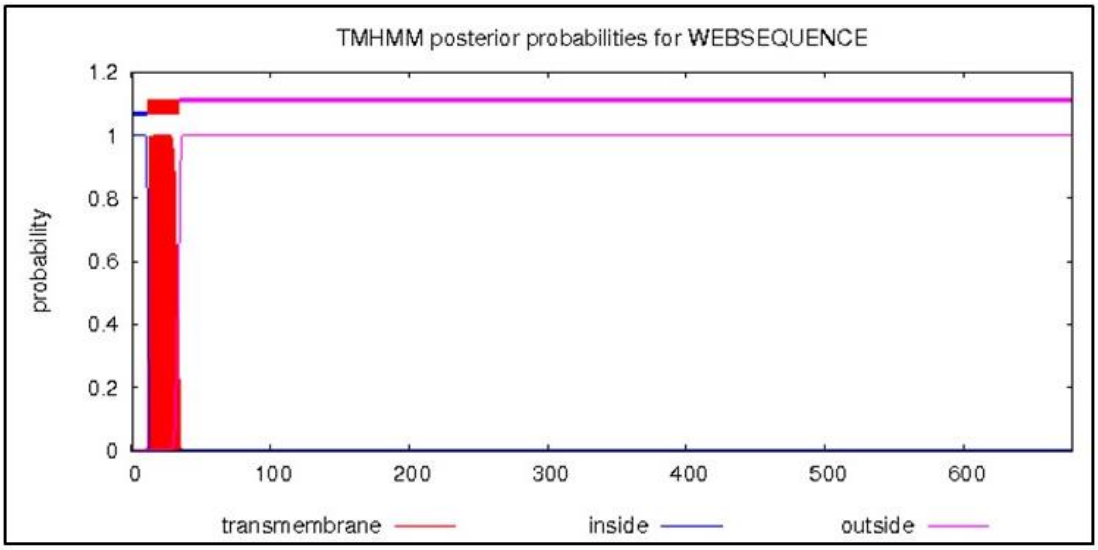

Figure 25: Program predictor displays the first 34 amino acid residues out of 678 amino acids to make up the transmembrane helix. Truncated version of PBP5 without the Transmembrane Helix and with the Hexa-Histidine Tag would result in a molecular weight of 72.3 kDa.

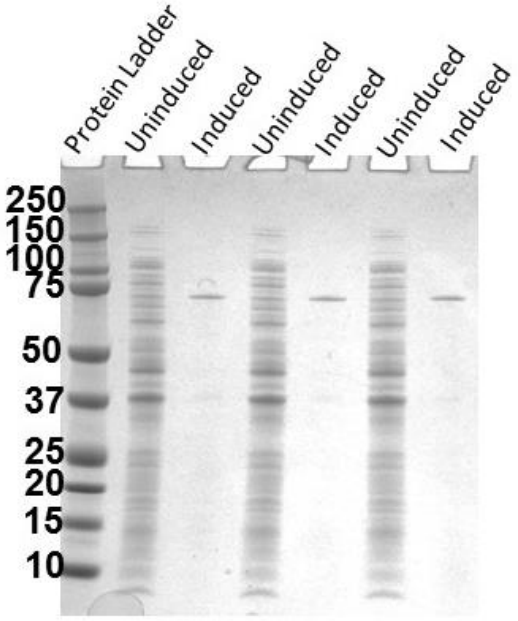

Figure 26: Test Expression Gel shows 3 different colonies of uninduced and induced BL21 E.Coli with PBP5. Molecular weight appears be as predicted from Figure 25, being around 72 kDa.

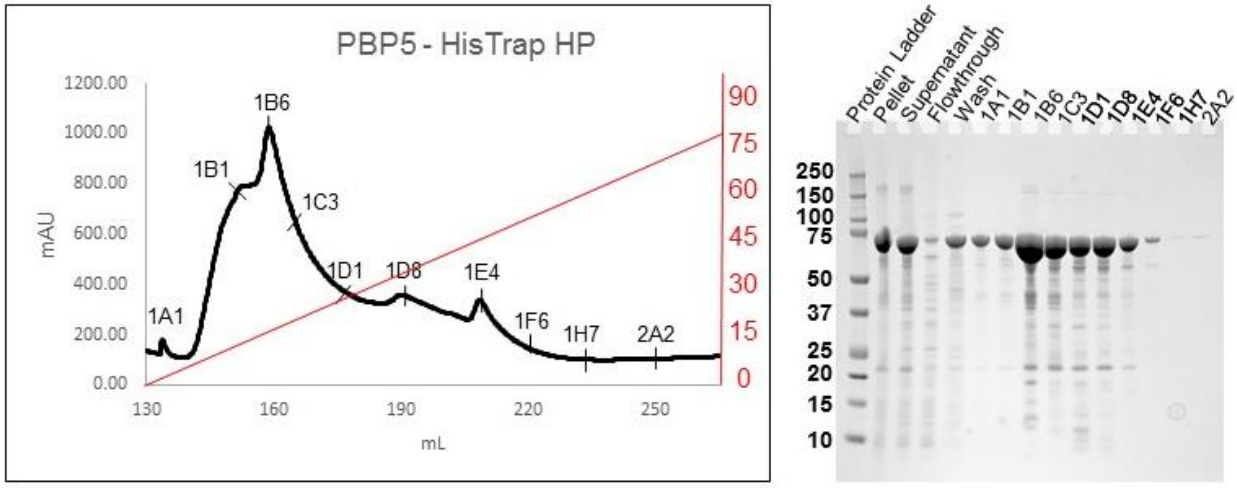

Figure 27: HisTrap Chromatography of His-Tagged PBP5. Elution was done with 500 mM Imidazole with a resulting yield typically ranging from 200 to 250 mg of protein after HisTrap Purification. SDS Page Gel also displays desired protein at the expected molecular weight.

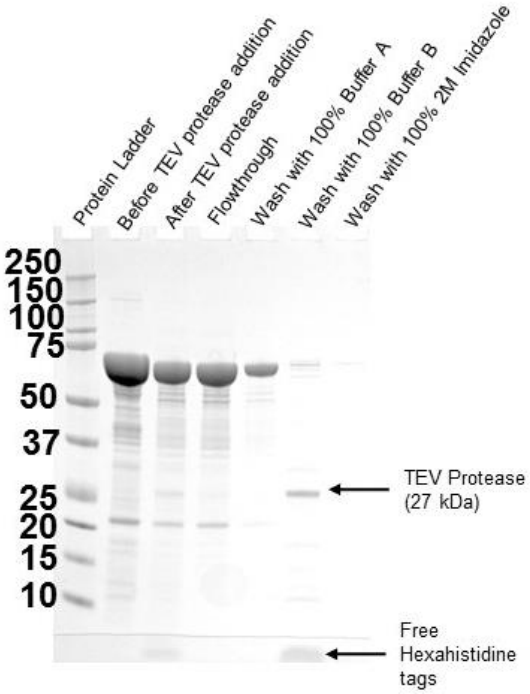

Figure 28: SDS Page Gel showing TEV Protease activity of cleaving the Hexahistidine tag from desired protein. TEV Protease and the free flowing Hexahistidine tags are labeled in the figure above.

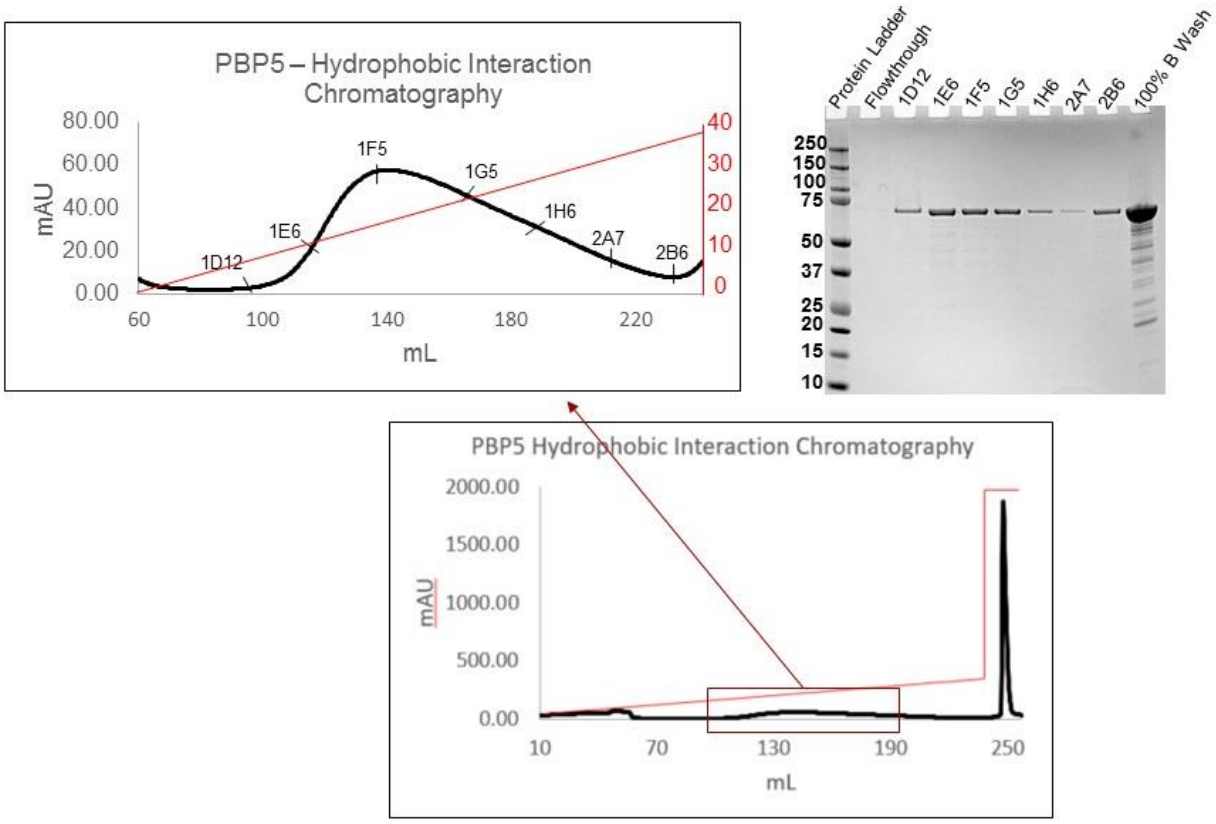

Figure 29: Hydrophobic Interaction Chromatography resulted in 20% recovery of pure protein. Towards the end of purification, we observed protein that is presumed to be denatured in some fashion or other E.Coli proteins that were not separated via Nickel Subtraction.

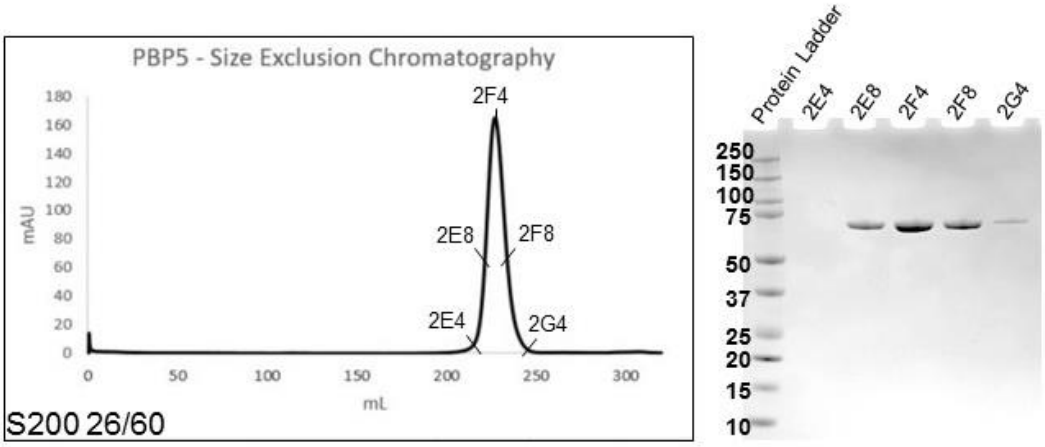

Figure 30: Size Exclusion Chromatography was done as with a Superdex 200 Column where elution occurred at 225 mL, which corresponds to molecular weight standards. SDS Page gel indicates 100% purity.

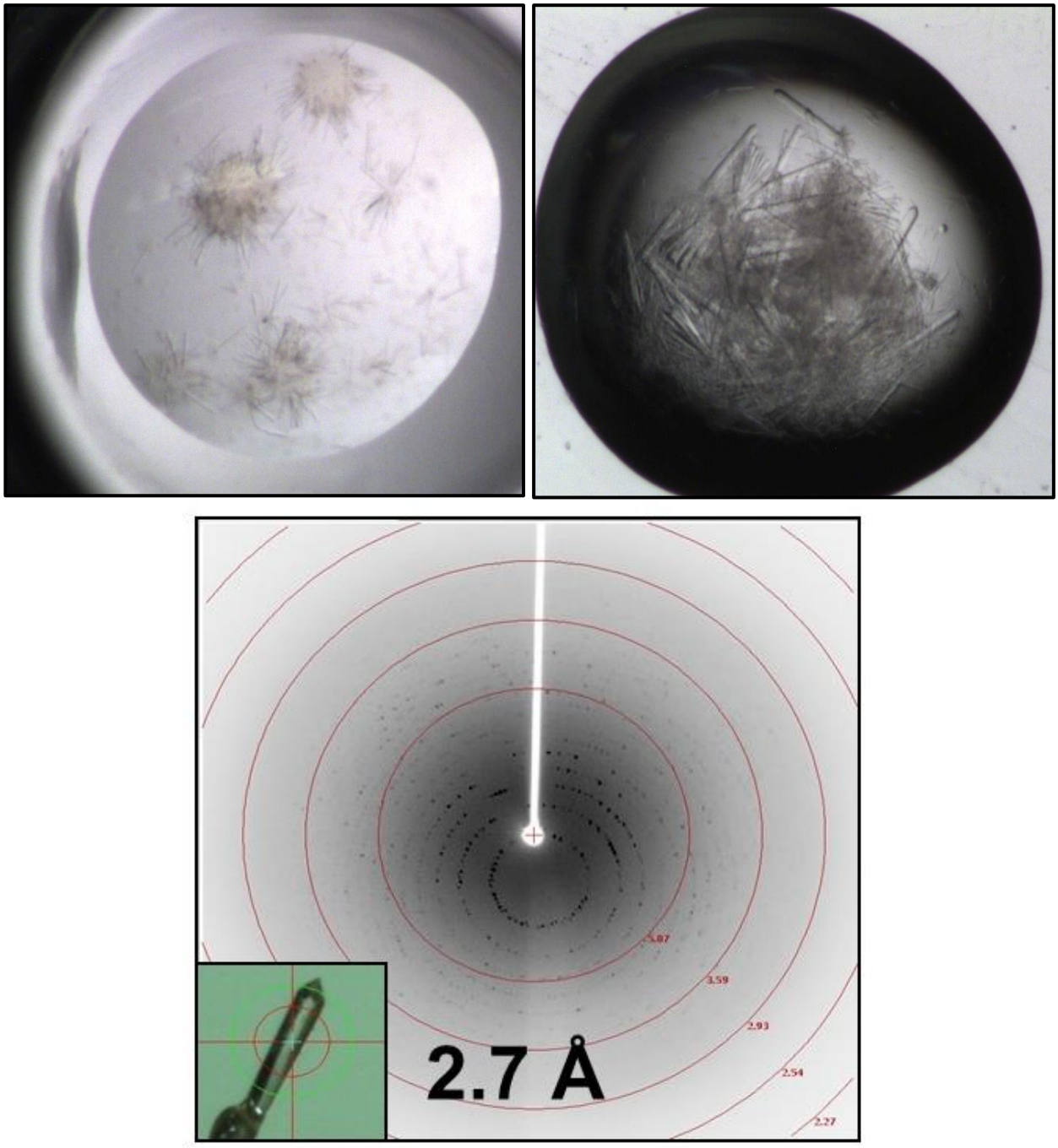

Figure 31: After crystallization trials, we observed crystals to grow in the commercial crystal screen Wizard 1 & 2 at the following condition: 2.0 M Ammonium Sulfate, 0.1 M Citrate pH 5.5. Crystals were grown at a larger scale by hanging drop setup and cryoprotected in 5.0 M Ammonium Sulfate. Strong reflections extended to 2.9 Å.

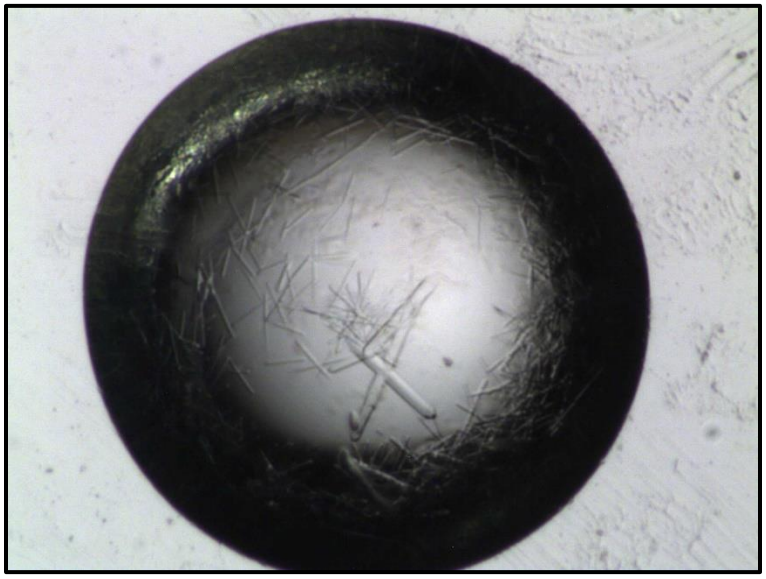

Figure 32: PBP5 and Penicillin G were mixed at a 1:10 molar ratio for cocrystallization. Crystals emerged from hanging drop setup after 2 weeks.

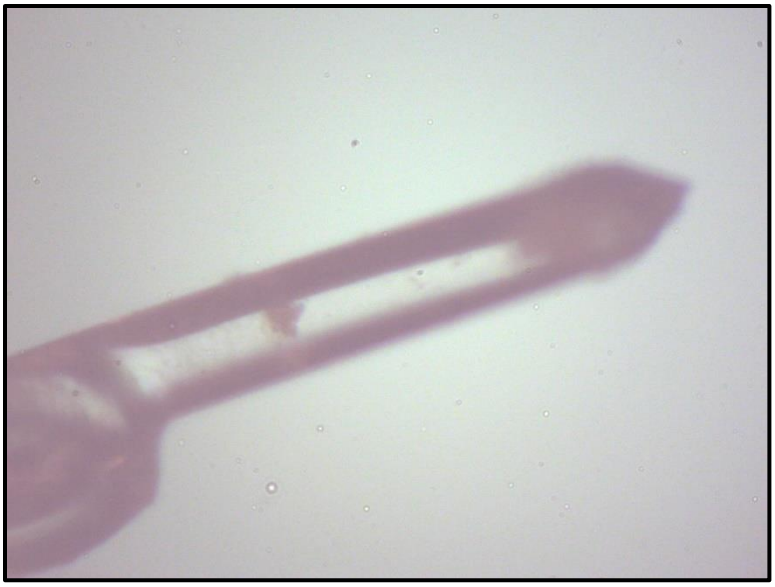

Figure 33: PBP5 apo crystals were soaked with Imipenem at a 1:10 and 1:20 molar ratio. Crystals continued to remain stabilized before data collection.

	PBP5 *apo*	PBP5 + benzylpenicillin	PBP5 + Imipenem
Data collection			
Space group	$P6_322$	$P6_322$	$P6_322$
Cell dimensions			
a, *b*, *c* (Å)	190.5, 190.5, 156.5	192.3, 192.3, 156.1	192.9, 192.9, 155.9
α, β, γ (°)	90, 90, 120	90, 90, 120	90, 90, 120
Resolution (Å)	38 - 2.7 (2.8 - 2.7)[a]	38.2 – 2.9 (3.0-2.9)	29.8 - 2.8 (2.9-2.8)
$R_{merge,}$	0.059 (0.445)	0.242 (2.67)	0.157 (1.66)
R_{meas}	0.080 (0.613)	0.279 (3.09)	0.166 (1.80)
$I/\sigma(I)$	13.0 (2.5)	9.2 (1.7)	20.1 (1.8)
$CC_{1/2}$	0.997 (0.707)	0.991 (0.379)	0.999 (0.334)
Completeness	0.98 (0.98)	0.99 (0.98)	0.99 (0.98)
Redundancy	3.1 (3.2)	7.5 (7.5)	18.3 (12.9)
Refinement			
Resolution (Å)	38.1 – 2.7	38.2-2.9	29.8 – 2.8
Total no. reflections	143438	274980	777376
No. unique reflections	45732	36580	42418
R_{work} / R_{free}	0.18/0.21	0.19/0.21	0.18/0.22
No. atoms	4945	4929	4731
Protein	4814	4809	4661
Ligand/ion (specify/describe)	71	14	45
Water	61	-	28
B factors			
Protein	57.9	67.8	72.5
Ligand/ion	88.5	93.6	79.3
Water	44.2	-	54.6
R.m.s. deviations			
Bond lengths (Å)	0.010	0.004	0.007
Bond angles (°)	1.05	0.64	0.86

Number of crystals for each structure should be noted in footnote.
[a] Values in parentheses are for highest-resolution shell.

Figure 34: X-ray Table of Solve Structure. Data collection and refinement statistics after molecular replacement.

GHMQETQAVEAGEKTVEQFVQALNKGDYNKAAEMTSKKAANKSALSEKEILDKYQ
NIYGAADVKGLQISNLKVDKKDDSTYSFSYKAKMNTSLGELKDLSYKGTLDRNDGQ
TTINWQPNLVFPEMEGNDKVSLTTQEAARGNIIDRNGEPLATTGKLKQLGVVPSKLG
DGGEKTANIKAIASSFDLTEDAINQAISQSWVQPDYFVPLKIIDGATPELPAGATIQEV
DGRYYPLGEAAAQLIGYVGDITAEDIDKNPELSSNGKIGRSGLEMAFDKDLRGTTGG
KLSITDADGVEKKVLIEHEVQNGKDIKLTIDAKAQKTAFDSLGGKAGSTVATTPKTGD
LLALASSPSYDPNKMTNGISQEDYKAYEENPEQPFISRFATGYAPGSTFKMITAAIGL
DNGTIDPNEVLTINGLKWQKDSSWGSYQVTRVSDVSQVDLKTALIYSDNIYTAQETL
KMGEKKFRTGLDKFIFGEDLDLPISMNPAQISNEDSFNSDILLADTGYGQGELLINPIQ
QAAMYSVFANNGTLVYPKLIADKETKDKKNVIGETAVQTIVPDLREVVQDVNGTAHSL
SALGIPLAAKTGTAEIKEKQDVKGKENSFLFAFNPDNQGYMMVSMLENKEDDDSAT
KRASELLQYLNQNYQ

Figure 35: Above is the resulting amino acid sequence of PBP5 after all purification has reached completion. The final molecular weight is predicted to be 70045.36 Da, which will be a necessary value for Mass Spectrometry Data Analysis.

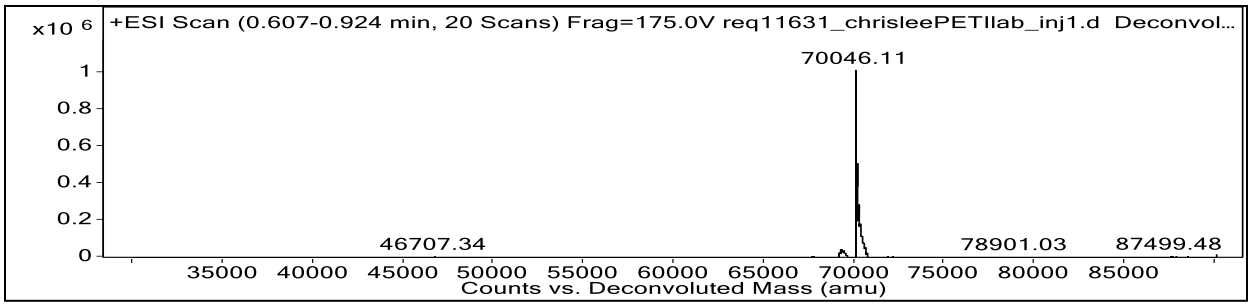

Figure 36: Mass spectrometry was the chosen method for observing antibiotic covalent binding to PBP5. Mass spectrometry displays average mass of our sample; therefore, determining whether antibiotics are covalently bound to PBP5 is a matter of adding the molecular weight of the given antibiotic to the average mass measured. The above displays measured molecular weight of PBP5 at 700046.11 Da, which displays data accuracy as our expected molecular weight is 70045.36 Da.

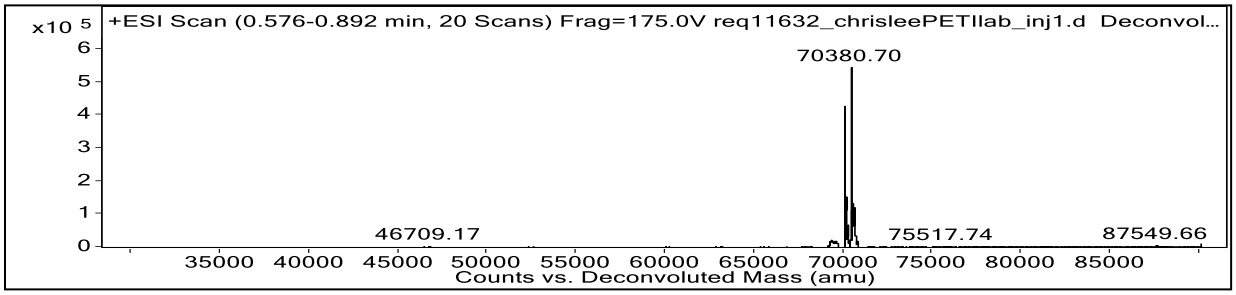

Figure 37: Mass spectrometry data of PBP5 with Penicillin G in a 1 to 10 molar ratio where sampels were incubated for 2 hours before testing. Data displays partial binding where the smaller peak is representative of PBP5 apo. However, the larger peak indicates the mass of a PBP5:Penicillin G complex. Measured molecular weight of the complex is 70380.70 Da while the expected molecular weight after calculation is 70380.51 Da.

a)

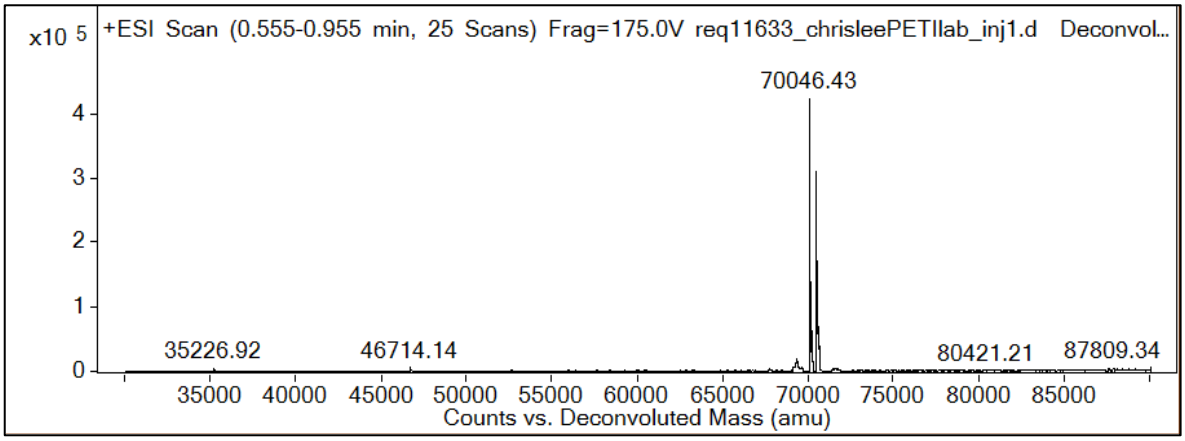

b)

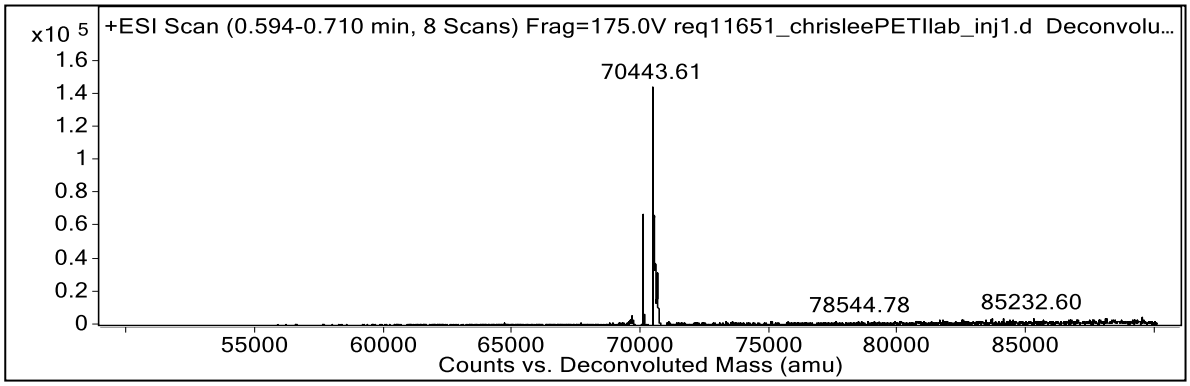

c)

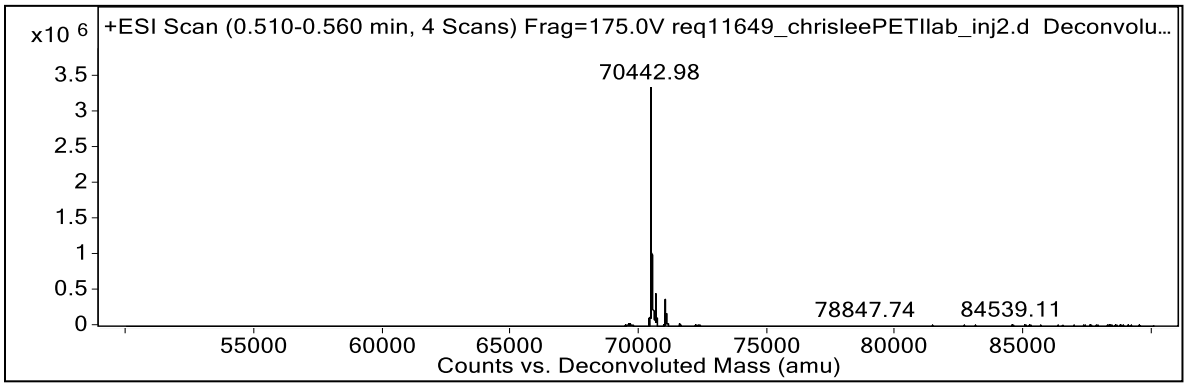

Figure 38: a) For the PBP5:Ceftriaxone complex, we ran the same method of sample preparation as conducted for PBP5:Penicillin G, mixing at a 1 to 10 molar ratio with incubation for 2 hours. With the molecular weight of ceftriaxone being 661.10 g/mol, we were looking for a mass around 70,700 Da. However, our sample showed partial binding where the larger peak was more representative of PBP5 alone and the smaller peak showed a molecular weight of 70,440 Da. However, the issue was resolved by increasing the molar ratio and increasing the time of incubation. Figure 38b) displayed data of sample mixed at a 1 to 100 molar ratio. Figure 38c) displayed data of sample mixed at a 1 to 1000 molar ratio.

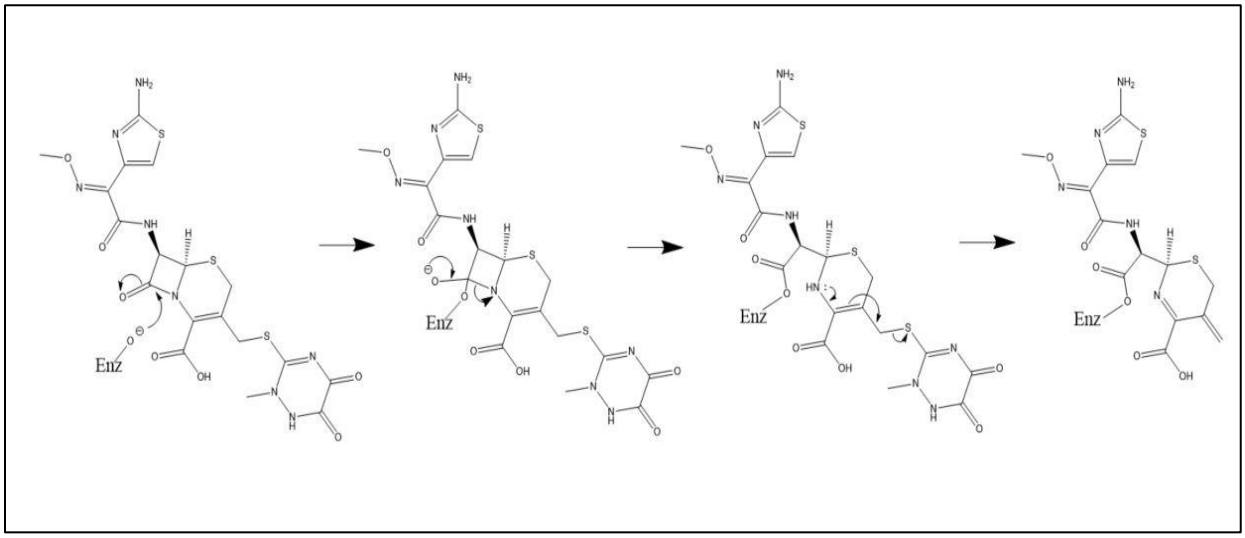

Figure 39: Curved arrow mechanism of active site serine interacting with the inactive form of Ceftriaxone, resulting in a large sulfate leaving group and reduced molecular of the active form of ceftriaxone. Inactive to active Ceftriaxone reduces molecular weight from 661.60 g/mol to 397.43 g/mol.

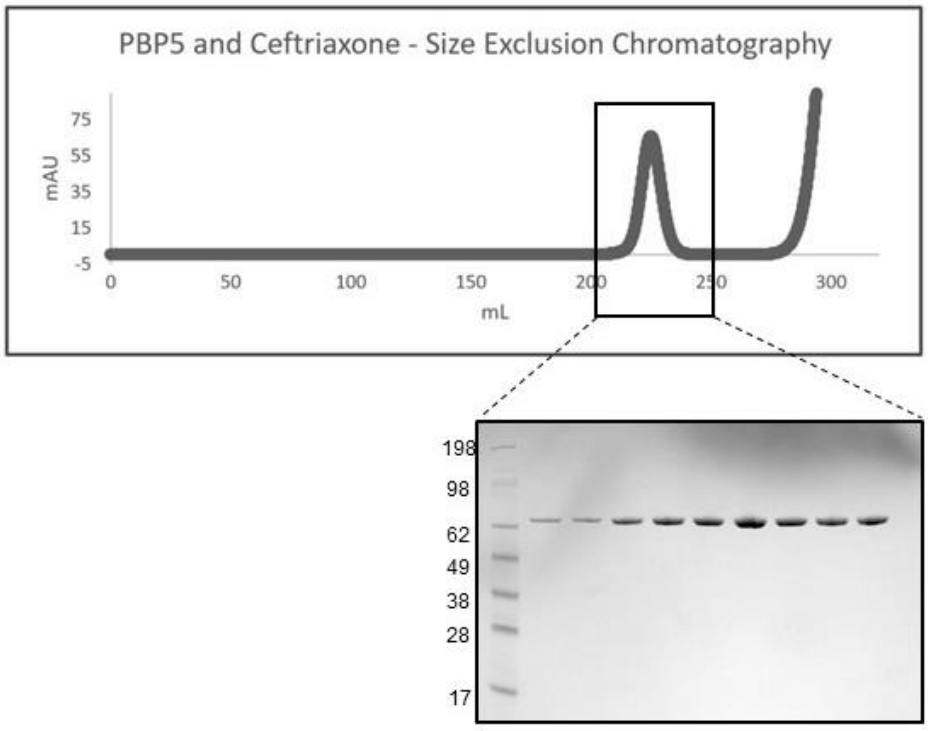

Figure 40: A second size exclusion chromatography step was performed after an overnight incubation of the PBP5:Ceftriaxone mixture at a 1:1000 protein to antibiotic molar ratio. SDS Page Gel displays 100% purity of our complex. Chromatogram also demonstrates clear separation of our complex with excess ceftriaxone towards the end of elution.

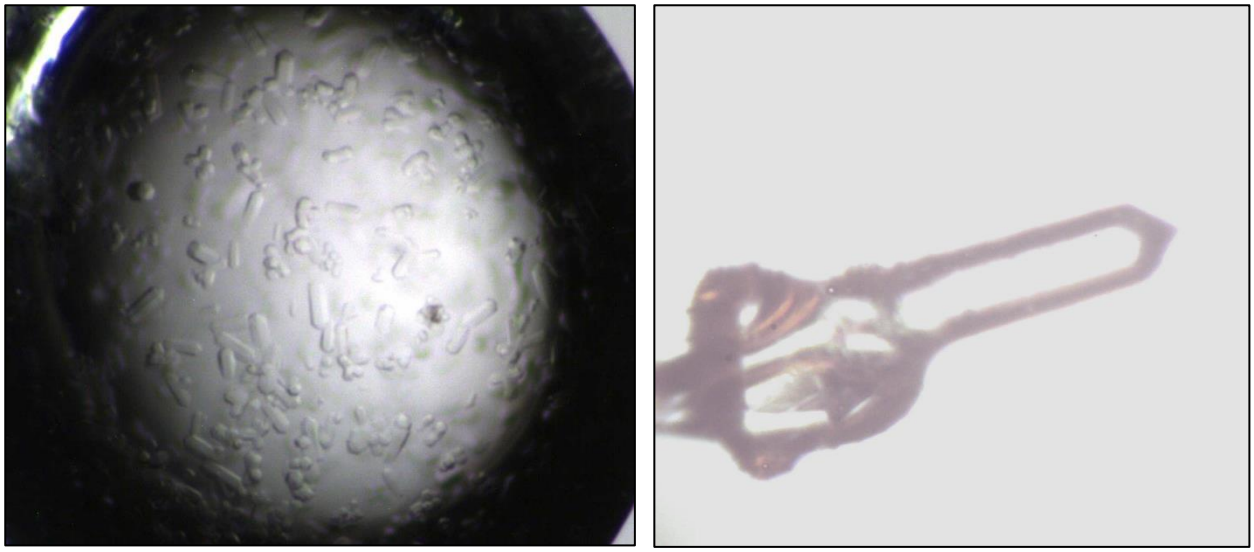

Figure 41: Pure samples were screened against personally designed Ammonium Sulfate Grid Screen with crystals emerging at 2.6 M Ammonium Sulfate, 0.1 BICINE pH 9. Crystals formed in a hexagonal morphology and generated poor diffraction data. Further trials would be required.

References

1. Rossolini GM, Arena F, Pecile P, Pollini S. Update on the antibiotic resistance crisis. *Clin Opin Pharmacol*. 2014; 1856-60.
2. Michael CA, Dominey-Howes D, Labbate M. The antibiotic resistance crisis: causes, consequences, and management. *Front Public Health* 2014; 2: 145.
3. Chan, M. "Antimicrobial resistance in the European Union and the world." G7 Helath Ministers Meeting, October 2015, Berlin, Germany. World Health Organization.
4. Runcie, H. "Infection in a Pre-Antibiotic Era." *J anc Dis Prev Rem.* 2015; 3: 125.
5. Ventola, C. Lee. "The Antibiotic Resistance Crisis: Part 1: Causes and Threats." *Pharmacy and Therapeutics* 2015; 40 (4): 277–283.
6. Fraser F, Dew JW, Taylor DC, Dennis AW, Oliver MWB, *et al*. "Primary and Delayed Primary Suture of Gunshot Wounds." *Brit J Surg* 1918; 19: 92-124.
7. Pettit RT. "Infections of Wounds of War with special reference to Gas Gangrene." *J Amer Med Assoc.* 1919; 73: 494-496.
8. Fleming A. "On the antibacterial action of cultures of a penicillium, with special reference to their use in the isolation of B. influenzae." *British Journal of Experimental Pathology.*1929; 10: 226-236.
9. Spellberg B, Gilbert DN. "The future of antibiotics and resistance: a tribute to a career of leadership by John Bartlett." *Clin Infect Dis.* 2014; 59 suppl 2:S71–S75.
10. "The antibiotic alarm." *Nature.* 2013; 495 (7440): 141
11. Bartlett JG, Gilbert DN, Spellberg B. "Seven ways to preserve the miracle of antibiotics." *Clin Infect Dis.* 2013; 56 (10): 1445–1450.
12. O'Neill J. "Antimicrobial resistance: tackling a crisis for the health and wealth of nations*." Rev Antimicrob Resist.* 2014.
13. Gross M. "Antibiotics in crisis." *Curr Biol.* 2013; 23 (24): R1063–R1065.
14. Sengupta S, Chattopadhyay MK, Grossart HP. "The multifaceted roles of antibiotics and antibiotic resistance in nature." *Front Microbiol*. 2013; 4: 47.
15. Williamson, R., C. LaBouguenec, L. Gutmann, and T. Horaud. "One or two low affinity penicillin-binding proteins may be responsible for the range of susceptibility of *Enterococcus faecium* to penicillin." *J. Gen. Microbiol*. 1985; 131: 1933-1940.
16. Grayson, M L et al. "Increasing Resistance to Beta-Lactam Antibiotics among Clinical Isolates of Enterococcus Faecium: A 22-Year Review at One Institution." *Antimicrobial Agents and Chemotherapy* 1991; 35 (11): 2180–2184.
17. Pauline Macheboeuf, Carlos Contreras-Martel, Viviana Job, Otto Dideberg, Andréa Dessen. "Penicillin Binding Proteins: key players in bacterial cell cycle and drug resistance processes." *FEMS Microbiol Rev.* 2006; 30 (5): 673-691.
18. Fisher, J. F., and S. Mobashery. "Three decades of the class A β-lactamase acyl-enzyme." *Curr. Protein Pept. Sci*. 2009; 10:401-407.
19. Bayles, K. W. "The bactericidal action of penicillin: new clues to an unsolved mystery." *Trends Microbiol.* 2000; 8: 274-278.
20. Bowler, L. D., Q. Y. Zhang, J. Y. Riou, and B. G. Spratt. "Interspecies recombination between the *penA* genes of *Neisseria meningitidis* and commensal *Neisseria* species during the emergence of penicillin resistance in *N. meningitidis*: natural events and laboratory simulation." *J. Bacteriol.* 1994; 176: 333-337.

21. Page, M. G. “Resistance mediated by penicllin-binding proteins” *ASM Press.* 2007; 81-99.
22. Chambers, H. F. “Penicillin-binding protein-mediated resistance in pneumococci and staphylococci.” *J. Infect. Dis*. 1999; 179 (Suppl. 2):S353-S359.
23. Gupta, Radhey S. “Origin of Diderm (Gram-Negative) Bacteria: Antibiotic Selection Pressure rather than Endosymbiosis Likely Led to the Evolution of Bacterial Cells with Two Membranes.” *PMC.* 2011; 100 (2): 171–182.
24. Chain E. “The early years of the penicillin discovery.” *Trends Pharmacol Sci J.* 1979; 1: 6–11
25. Abraham EP, Chain E, Florey HW, Florey ME, Heatley NG, Jennings MA, *et al.* “Historical introduction." In: Florey HW, Heatley CE, Jennings NG, Sanders MA, Abraham AG, Florey EPME, editors. *Antibiotics*. London: Oxford University Press. 1949
26. Lundberg, M.; Siegbahn, P. E. M.; Morokuma, K. "The Mechanism for Isopenicillin N Synthase from Density-Functional Modeling Highlights the Similarities with Other Enzymes in the 2-His-1-carboxylate Family†". *Biochemistry.* 2008; 47 (3): 1031–1042.
27. Sauvage, E., Charlier P., Terrak M., and JA. Ayala. “The penicillin-binding proteins: structure and role in peptidoglycan biosynthesis.” *FEMS Microbiol Rev*. 2008; 32 (3): 234-58.
28. Höltje JV. “Growth of the stress-bearing and shape maintaining murein sacculus of *Escherichia coli.” Microbiol Mol Biol Rev* 1998; 62: 181–203.
29. den Blaauwen T, de Pedro M, Nguyen-Diste`che M & Ayala J. “Morphogenesis of rod-shaped sacculi.” *FEMS Microbiol Rev* 2008; 32: 321–344.
30. Zapun A, Vernet T & Pinho M. “The different shapes of cocci.” *FEMS Microbiol Rev* 2008; 32: 345–360.
31. Meeske, A. J. *et al. “*SEDS proteins are a widespread family of bacterial cell wall polymerases.” *Nature* 2016; 537, 634–638.
32. Cho, H. *et al. “*Bacterial cell wall biogenesis is mediated by SEDS and PBP polymerase families functioning semi-autonomously.” *Nature Microbiol.* http://dx.doi. org/10.1038/nmicrobiol.2016.172 (2016).
33. McPherson, D. C. & Popham, D. L. “Peptidoglycan synthesis in the absence of class A penicillin-binding proteins in Bacillus subtilis.” *J. Bacteriol.* 2003; 185, 1423–1431.
34. Arbeloa, A. *et al “*Role of class A penicillin-binding proteins in PBP5-mediated beta-lactam resistance in Enterococus faecalis*.” J. Bacteriol.*2004*:* 186, 1221–1228.
35. Vollmer W, Joris B, Charlier P & Foster S “Bacteria peptidoglycan (murein) hydrolases.” *FEMS Microbiol Rev* 2008; 32: 259–286.
36. Spratt BG & Strominger JL. “Identification of the major penicillin-binding proteins of Escherichia coli as D-alanine carboxypeptidase IA.” *J Bacteriol* 1976; 127: 660–663.
37. Lim D & Strynadka NC. “Structural basis for the beta lactam resistance of PBP2a from methicillin-resistant Staphylococcus aureus.” *Nat Struct Biol* 2002; 9: 870–876.
38. Ghuysen JM. “Serine beta-lactamases and penicillin binding proteins.” *Annu Rev Microbiol* 1991; 45: 37–67.
39. Goffin C & Ghuysen JM. “Multimodular penicillin-binding proteins: an enigmatic family of orthologs and paralogs.” *Microbiol Mol Biol Rev* 1998; 62: 1079–1093.
40. Goffin C Ghuysen JM. “Biochemistry and comparative genomics of Sxxk superfamily acyltransferases offer a clue to the mycobacterial paradox: presence of penicillin-

susceptible target proteins versus lack of efficiency of penicillin as therapeutic agent." *Microbiol Mol Biol Rev* 2002; 66: 702-738.
41. Nicola G, Peddi S, Stefanova M, Nicholas RA, Gutheil WG & Davies C. "Crystal structure of Escherichia coli penicillinbinding protein 5 bound to a tripeptide boronic acid inhibitor: a role for Ser-110 in deacylation." *Biochemistry* 2005; 44: 8207–8217.
42. Otero, Lisandro H. *et al*. "How Allosteric Control of *Staphylococcus Aureus* Penicillin Binding Protein 2a Enables Methicillin Resistance and Physiological Function." *Proceedings of the National Academy of Sciences of the United States of America* 2013; 110 (42): 16808–16813.
43. Enright MC, *et al.* "The evolutionary history of methicillin-resistant Staphylococcus aureus (MRSA)." *Proc Natl Acad Sci USA* 2002; 99 (11): 7687-7692.
44. Arbeloa, Ana *et al.* "Role of Class A Penicillin-Binding Proteins in PBP5-Mediated B-Lactam Resistance in *Enterococcus Faecalis*." *Journal of Bacteriology* 2004; 186 (5): 1221–1228.
45. Duez, C., W. Zorzi, F. Sapunaric, A. Amoroso, I. Thamm, and J. Coyette. "The penicillin resistance of*Enterococcus faecalis* JH2-2r results from an overproduction of the low-affinity penicillin-binding protein PBP4 and does not involve a *psr*-like gene." *Microbiology* 2001; 147: 2561-2569.
46. Fontana, R., M. Aldegheri, M. Ligozzi, H. Lopez, A. Sucari, and G. Satta. "Overproduction of a low-affinity penicillin-binding protein and high-level ampicillin resistance in *Enterococcus faecium." Antimicrob Agents Chemother* 1994; 38:1980-1983.
47. Sifaoui, F., M. Arthur, L. Rice, and L. Gutmann. "Role of penicillin-binding protein 5 in expression of ampicillin resistance and peptidoglycan structure in *Enterococcus faecium. Antimicrob Agents Chemother.* 2001; 45: 2594-2597.

Other Figures

F.1. van Heijenoort J. "Recent advances in the formation of the bacterial peptidoglycan monomer unit." *Nat Prod Rep* 2001; 18: 503–519.
F.2. Zeng X, Lin J. "Beta-lactamase induction and cell wall metabolism in Gram-negative bacteria." *Front Microbiol* 2013; 4.
F.3. King D. T., Lameignere E. & Strynadka N. C. "Structural insights into the lipoprotein outer membrane regulator of penicillin-binding protein 1B." *J. Biol. Chem.* 2014; 289, 19245–19253.
F.4. Lim D., Strynadka N. C. J. "Structural basis for the beta-lactam resistance of PBP2a from methicillin-resistant *Staphylococcus aureus*." *Nat. Struct. Biol* 2002; 9, 870–876.
F.5. Rajashankar KR, Ray SS, Bonanno JB, Burley SK. "Crystal structure of penicillin-binding protein 4 (Pbp4) from *Staphylococcus aureus*." PDB: 1TVF.
http://www.ncbi.nlm.nih.gov/Structure/mmdb/mmdbsrv.cgi?form=6&db=t&Dopt=s&uid=28361
F.6. Lovering A. L., de Castro L. H., Lim D. & Strynadka N. C. "Structural insight into the transglycosylation step of bacterial cell-wall biosynthesis." *Science*. 2007; 315, 1402–1405.
F.7. Sauvage E, Duez C, Herman R, Kerff F, Petrella S, Anderson J, Adediran S, Pratt F, Frère J, Charlier P. "Crystal structure of the *Bacillus subtilis* penicillin-binding protein 4a, and its complex with a peptidoglycan mimetic peptide." *J Mol Biol*. 2007; 371: 528–39.